Beta-band Motor Unit Coherence and Nonlinear Surface EMG Features of the First Dorsal Interosseous Muscle Vary with Force

Running title (40): Beta-Band Coherence Varies with Muscle Force

Keywords: motor unit, coherence, EMG, sample entropy, determinism

Author contributions: All experiments were performed in the Neuromuscular Systems Laboratory in University College Dublin, Ireland. L.M. and M.M.L. conceived and designed research; L.M. performed experiments; L.M., M.W.F. and M.M.L. analyzed data; L.M. and M.M.L. interpreted results of experiments; L.M. prepared figures; L.M. and M.M.L. drafted manuscript; L.M., M.W.F. and M.M.L. edited and revised manuscript; L.M., M.W.F. and M.M.L. approved final version of manuscript.

Corresponding Author: Dr Lara McManus

School of Electrical and Electronic Engineering,

University College Dublin, Belfield, Dublin 4, Ireland

lara.mc-manus@ucdconnect.ie

Other Authors: Dr Matthew W. Flood

School of Electrical and Electronic Engineering,

University College Dublin, Belfield, Dublin 4, Ireland

matthew.flood@ucdconnect.ie

Prof. Madeleine M. Lowery

School of Electrical and Electronic Engineering,

University College Dublin, Belfield, Dublin 4, Ireland

madeleine.lowery@ucd.ie

Details of Funding: European Research Council: ERC-2014-CoG-646923_DBSModel

Abstract

Motor unit (MU) firing times are weakly coupled across a range of frequencies during voluntary contractions. Coherent activity within the beta-band (15-35 Hz) has been linked to oscillatory cortical processes, providing evidence of functional connectivity between the motoneuron pool and motor cortex. The aim of this study was to investigate whether beta-band MU coherence is altered with increasing abduction force in the first dorsal interosseous muscle. Coherence between MU firing times, extracted from decomposed surface EMG signals, was investigated in 17 subjects at 10%, 20%, 30% and 40% of maximum voluntary contraction. Corresponding changes in nonlinear surface EMG features, specifically sample entropy and determinism which are sensitive to MU synchronization, were also examined. A reduction in beta-band and alpha-band coherence was observed as force increased ($F(3, 151) = 32$, $p < .001$ and $F(3, 151) = 27$, $p < .001$, respectively), accompanied by corresponding changes in nonlinear surface EMG features. A significant relationship between the nonlinear features and MU coherence was also detected ($r = -0.43 \pm 0.1$ and $r = 0.45 \pm 0.1$, for sample entropy and determinism, respectively, both $p < .001$). The reduction in beta-band coherence suggests a change in the relative contribution of correlated and uncorrelated pre-synaptic inputs to the motoneuron pool, and/or a decrease in the responsiveness of the motoneuron pool to synchronous inputs at higher forces. The study highlights the importance of considering muscle activation when investigating changes in MU coherence or nonlinear EMG features, and examines other factors that can influence coherence estimation.

New and Noteworthy (75 words)

Intramuscular alpha- and beta-band coherence decreased as muscle contraction force increased. Beta-band coherence was higher in groups of high threshold motor units than in simultaneously active lower threshold units. Alterations in motor unit coherence with increases or decreases in force and with the onset of fatigue were accompanied by corresponding changes in surface EMG sample entropy and determinism. Mixed model analysis indicated mean firing rate and number of motor units also influenced the coherence estimate.

Introduction

During voluntary contraction, the discharge of motor units within a muscle is not completely independent and motor units exhibit a weak tendency to fire within a few milliseconds of one another, with a rate of occurrence above that expected due to chance. Short-term motor unit synchrony is particularly prominent in distal finger and hand muscles, which receive direct monosynaptic connections from corticomotoneuronal cells (Porter and Lemon 1993). Indirect evidence of functional connectivity between the motor cortex and the motoneuron pool is provided by studies investigating corticomuscular coherence, which have shown that motor unit firing is temporally correlated with oscillatory cortical activity within the beta frequency range (15 – 30 Hz) during steady muscle contractions (Conway et al. 1995). Time and frequency domain analysis of the firing times of pairs of motor units has revealed the presence of two neural components, one responsible for 15 – 30 Hz coherence and short-term motor unit synchronization, and another component in the 1 – 12 Hz frequency range, unrelated to short-term synchronization (Farmer et al. 1993). Coherence between motor unit firing times is likely to be influenced by a number of factors (Kirkwood 2016), these include the strength of shared beta oscillatory activity among pre-synaptic inputs (functional common input) and the anatomical organisation of shared inputs to the motoneuron (structural organisation). Although the overall motor unit coherence estimate is not a direct measure of the magnitude of synchronized motoneuron inputs, variations in coherent beta-band activity may reveal concurrent changes in the properties of synaptic inputs to the motoneuron pool.

While corticomuscular and motor unit coherence have been examined under a range of different conditions, it has not yet been established whether there is a systematic change in the magnitude of beta-band motor unit coherence with increases in the level of muscle activation. Beta-band corticomuscular coherence has been observed to decrease at higher forces during isometric contractions in the tibialis anterior, the first dorsal interosseous (FDI) and knee extensors and flexors (Dal Maso et al. 2017; Perez et al. 2012; Ushiyama et al. 2012). In contrast it was found to be unchanged with increasing force in the soleus, abductor pollicis brevis and biceps (Mima and Hallett 1999; Ushiyama et al. 2012), and to increase with contraction strength in the FDI at very low forces (Kilner et al. 2000; Witte et al. 2007). While several studies have observed a change in corticomuscular coherence, the majority of those investigating coherent beta-band activity in the firing times of motor units within a muscle have not detected a corresponding change with increasing contraction intensity (Castronovo et al. 2015; Christou et al. 2007; Schmied and Descarreaux 2011), though a higher incidence of significant coherence has been reported (Laine et al. 2015). Conflicting findings have been described in studies assessing variations in motor unit short-term synchronization, which is directly related to beta-band

coherence (Farmer et al. 1993; Lowery et al. 2007; Semmler et al. 2002). At higher forces, motor unit synchronization strength has been reported to decrease (Kline and De Luca 2015; Nordstrom et al. 1992), increase (Schmied and Descarreaux 2010), show no systematic trend (Christou et al. 2007), or exhibit disparate changes with different synchrony indices (Fling et al. 2009). These earlier studies on motor unit coherence and synchronization have been largely limited to very low force levels in order to reliably discriminate motor units as the contraction intensity increases. Recent advances in surface EMG decomposition enable motor unit activity across a wider range of force levels to be investigated, and yields information on a greater number of concurrently active motor units than traditional intramuscular EMG methods. Compared with estimates from paired motor unit recordings, coherence analysis of a larger motor unit sample using composite spike trains has the potential to enhance the detection of correlated motor unit discharges (Farina et al. 2014). Furthermore, quantifying coherent motor unit activity within the same muscle may provide a more accurate assessment of synchrony at the whole muscle level when compared with corticomuscular and inter-muscular recordings.

The primary aim of this study was to examine whether beta-band motor unit coherence in the FDI muscle changes systematically with increasing index finger abduction force between 10% and 40% MVC. Motor unit coherence was also investigated in the lower alpha-band (8 - 12 Hz), as synchronous motor unit activity has been observed in this range during slow finger movements and under isometric force conditions (Elble and Randall 1976; Farmer et al. 1993; Halliday et al. 1999; Semmler et al. 2003). It is reasonable to assume that the structure of the global surface EMG signal will also be affected by the degree of coherent activity in its constituent motor unit discharges. A secondary aim of this study was thus to establish whether changes in the underlying motor unit beta-band coherence are reflected in the nonlinear estimates of surface EMG signal complexity and deterministic structure, specifically the sample entropy (SampEn) and percentage determinism (%DET). These nonlinear measures characterise the degree of similarity and repeating structure within a signal (Richman and Moorman 2000; Webber et al. 1995), and have previously captured differences in surface EMG signals under conditions where normal motor unit synchronization is enhanced (Farina et al. 2002; Fattorini et al. 2005). However, experimental studies have not yet detected a significant relationship between these nonlinear surface EMG parameters and beta-band motor unit coherence (Schmied and Descarreaux 2011).

Methods

Index finger abduction force and EMG activity of the first dorsal interosseous muscle were recorded during isometric abduction of the index finger in seventeen young adults with no neurological conditions (8 female, age 28 ± 5 years, 2 left-handed, 1 ambidextrous or ambiguously handed). Written informed consent was obtained from all participants and the experiments were conducted in accordance with the standards set by the Declaration of Helsinki and were approved by Human Research Ethics Committee for Sciences at University College Dublin.

Experimental procedure

Participants were seated upright with their upper arm and hand comfortably resting in pronation on a support, which was securely mounted with magnetic stands to a heavy steel table. To standardize hand position and to minimize contributions of other muscles, the forearm and index finger were cast and the little, ring and middle fingers were separated from the index finger and strapped to the support surface. The thumb was secured at an approximately 60-degree angle to the index finger. The proximal phalanx of the index finger was fixed to a ring-mounted interface attached to two load cells (Interface, Inc., SML-110N) to record force generated in the abduction/adduction and extension/flexion directions. The magnitude and direction of the force generated, and the target force were presented on a screen positioned at eye-level. Surface EMG was recorded from the first dorsal interosseous muscle using a surface sensor array (Delsys, Inc.) that consisted of 5 cylindrical probes located at the corners and at the center of a 5 × 5 mm square (Nawab et al. 2010), and a reference electrode on the skin surface of olecranon. Pairwise differential recordings of the 5 electrodes yielded 4 channels of surface EMG, which were amplified and filtered between 20 Hz and 450 Hz. The signals were sampled at 20 kHz and stored on a computer for further processing. The force produced by the index finger was band-pass filtered between 0.5 and 30 Hz, and the root mean square error (RMSE) was calculated between the force generated in the abduction/adduction direction and the target force.

Maximal voluntary contraction (MVC) during isometric index finger abduction was determined for each subject as the highest force achieved during three short (3 s) maximum contractions, separated by a 1 min rest period, where the maximum force between trials lay within 10% of each other. Subjects then performed a series of isometric voluntary contractions, in which they were required to either maintain a constant abduction force or increase/decrease their force level by 10% MVC midway through the contraction. The constant force trials were performed at 10%, 20%, 30% and 40% MVC, the first half of the increasing force trials began at either 10%

or 20% MVC and the first half of decreasing force trials began at either 20% or 30% MVC. The total length of the force trajectory for each trial was 45 seconds, which included a 3 s quiescent period at the beginning and end of the trajectory for baseline noise calculation. Increases and decreases in the required force level were graded at a rate of 10% MVC/s. The protocol consisted of three repetitions of the constant force trials at 10% and 20% MVC, and two repetitions of the other constant force (30% MVC, 40% MVC) and the two-force level trials (10→20% MVC, 20→10% MVC, 20→30% MVC, 30→20% MVC). Subjects were occasionally required to perform additional repetitions to ensure that high force accuracy was obtained in at least one trial for each trajectory. Trials were performed in a randomized order, though consecutive high force contractions (i.e. 30% and 40% MVC) were avoided to minimize the development of fatigue. A minimum of 45 seconds of rest was provided between trials. Discriminable motor units (MUs) were extracted from the surface EMG signal using the decomposition EMG system (dEMG Analysis, version 1.1.3). The decomposition algorithm is outlined in detail in Nawab et al. (2010). For each detected MU, the output of the decomposition algorithm consisted of the MU firing times and 4 motor unit action potential (MUAP) waveforms corresponding to 4 pairs of bipolar electrode channels.

Motor unit acceptance criteria

The identified firing times for each MU were used to spike triggered average (STA) the surface EMG signal on each channel, resulting in 4 representative STA MUAP waveforms for each MU. The variation of the spike-triggered averaged MUAP template over time was quantified using a 4 s moving average window with 0.5 s time step. A MUAP template estimate was calculated based on the firing events in each window and the window was shifted along the length of the surface EMG signal, as performed in Hu et al. (2013). The STA templates were then examined in 4-dimensional space, with the co-ordinates of the 4-D trajectory provided by the MUAP waveform samples on each of the four channels. The trajectory of the estimated MUAP template for each window was compared to a reference trajectory, calculated as average template estimate across all windows. For a detected MU to be accepted for further analysis, a minimum of 75% of the trajectories obtained from the moving average window were required to lie within a fixed radius of the reference trajectory for that MU. Each accepted motor unit was also required to have a waveform trajectory distinct or separate from all other decomposed MUAP waveforms in 4-D space. To evaluate the separation or heterogeneity of the MUAP waveforms, the Euclidean distance between the trajectories of two detected motor units was calculated in 4-D for all possible pair combinations. Motor unit pairs with a distance less than -2.5 standard deviations from the mean were excluded from further analysis. In addition to

satisfying the requirements of trajectory stability and heterogeneity, motor units detected during the trials with two force levels were only accepted if their MUAP waveform trajectories were consistent across both force levels, indicating that the same motor unit was detected at both levels. Constant force trials were required to have a minimum of 12 accepted MUs, and two-force trials at least 8 accepted MUs to be included in the subsequent coherence analysis.

Due to the high level of motor unit superposition in surface EMG signals, when two or more motor units fire within a few milliseconds of one another, firing instances may have a higher likelihood of being missed in the decomposition of these signals compared with intramuscular EMG recordings. Missed co-incident firings will not be detected with coherence analysis, but a large quantity of missed synchronous firings could conceivably cause a reduction in coherence. Thus, an additional validation step was introduced to assess whether this limitation of surface EMG decomposition influenced the results. Cross-correlation histograms with 2 ms bins were constructed between pairs of firing trains for all forward and reverse times, to quantify the level of missed coincident firings in the decomposed motor unit data. A large number of missed co-incident firings between two motor units would be expected to manifest as a dip or "trough" at approximately zero lag in the cross-correlogram between their firing trains. The cross-correlogram for each pair was classified as belonging to one of three sub-groups: those that exhibited a trough, those that exhibited a broad or narrow peak typical of synchronous motor units, and those that did not show any distinct peaks in the correlogram. To assess whether missed firings could account for changes in coherence across the different force levels, the number of motor unit pairs exhibiting troughs in the cross-correlogram across all force levels was examined. Motor units that exhibited a trough in the cross-correlogram formed with more than 3 other motor units were removed and the coherence analysis was then repeated for the remaining motor units.

Coherence analysis

Motor unit activity was examined over 23 s, centered mid-way through the constant force trials, and during a 10 s period at each force level in the two-force trials. The middle section of each trajectory was chosen to exclude periods of motor unit recruitment and derecruitment during changes in force and at the start and end of each trial. The coherence within the motoneuron pool was estimated from pairs of composite spike trains (Farina et al. 2014; Negro and Farina 2011). The accepted motor units from each trial were divided into two groups, each containing an equal number of randomly chosen motor units. The firing trains in each group were summed to obtain two composite spike trains. The magnitude squared coherence between the two composite spike trains was calculated with 1s overlapping Hamming windows (nfft = 1024,

75% overlap, 86 segments for the single force trial and two sets of 36 segments for the two-force trials). This was repeated for 200 randomly chosen combinations of two groups from the same set of MUs, as each combination will generate a slightly different coherence estimate. Each trial was represented by the median coherence spectrum over all 200 combinations.

The Fisher "z-transform" was applied to the magnitude squared coherence estimates $C(f)$ to obtain a normally distributed variable $Z(f)$, Equation 1 (Enochson and Goodman 1965), with approximately unit variance (Halliday and Rosenberg 2000).

$$[1] \qquad Z(f) = \left[\sqrt{2\tilde{L}}\ \tanh^{-1}\left(\sqrt{C(f)}\right)\right]$$

Though the explicit formula for the statistical distribution of magnitude squared coherence with overlapping windows is not known, approximations are available (Gallet and Julien 2011). The number of disjoint segments (L) was substituted for the effective number of segments with 75% overlap ($\tilde{L}$) to calculate the variance and significance threshold for the transformed z-scores as described by Gallet and Julien (2011). The window function (w_l) and fixed delay (D, equal to 25% of the segment length) were used in the calculation of $\tilde{L}$. The 95% confidence limit (γ), Equation 5, was z-transformed to determine a significance threshold for the z-scores.

$$[2] \qquad c_w(D) = 1 + 2\sum_{j=1}^{L} \frac{L-j}{L} \rho_w^2(jD)$$

$$[3] \qquad \rho_w(M) = \frac{\sum_{t=0}^{L-M-1} w_l(t) w_l(t+M)}{\sum_{t=0}^{L-1} w_l(t)}$$

$$[4] \qquad \tilde{L} = \frac{L}{c_w(D)}$$

$$[5] \qquad \gamma = 1 - (0.05)^{1/(\tilde{L}-1)}$$

The mean coherence value in the 100 – 500 Hz range should theoretically be zero if there is no physiological coupling between the motor unit spike trains. However, in practice it has a small numerical value that can vary according to the degree of overlap, the spectral window function and number independent segments used. Therefore, for each trial the mean z-score in this range was subtracted from $Z(f)$ at all frequencies to remove this bias, as in Baker et al. (2003). The integral of significant values of $Z(f)$ was then calculated for each trial in the alpha (8-12 Hz) and beta-band frequency ranges (15-35 Hz). The value of the integral of the coherence in each frequency band was divided by the number of integration points in the frequency band.

The amplitude of each MUAP, an approximation of the motor unit size, was estimated as the distance traversed by the action potential in multidimensional space. To investigate whether there was a difference in the beta-band coherent activity of high and low threshold motor units, motor units were arranged in ascending order of size. The coherence for the first 8 motor units

was calculated between two composite pulse trains comprised of 4 MUs each. This was repeated for all combinations of two groups of 4 units (70 possible combinations), and the median coherence over all combinations was estimated. The coherence estimate for the first 8 motor units was then compared to that of the last 8 units for all trials (with at least 16 accepted motor units).

Nonlinear analysis

Before analysis, the surface EMG signal was lowpass filtered at 400 Hz (8^{th} order Chebyshev IIR filter) and downsampled to 1 kHz. Recurrence quantification analysis (RQA) was performed on non-overlapping 1.5 s segments of the surface EMG signal during the periods of constant force production in each trial. RQA involves transforming the single-channel surface EMG signal onto a multi-dimensional phase space trajectory, with each point on the trajectory representing a different point in time. This result is mapped onto a two-dimensional recurrence plot to provide a visualization of the times at which a phase space trajectory returns to a location in phase space that it has visited before. A recurrence represents a pair of points on the trajectory that are separated by a distance smaller than a specified radius value, and the recurrence plot depicts this result for all possible pairs of time points. The parameters selected in this study were chosen to effectively capture the dynamics of motor unit firing patterns (i.e. time delay = 1, embedding dimension =15, minimum diagonal line = 10 and radius = 0.2) (Flood et al. 2019; Marwan et al. 2007). Recurrence plots were used to calculate the percentage determinism (%DET, number of diagonal lines of consecutive points on the plot), a feature that illustrates how far the surface EMG signal is from a purely random signal (Webber et al. 1995). The median value over all channels and segments was taken as the representative %DET value. The median frequency and the root-mean-square amplitude of the surface EMG signal were calculated over the same sections of the signal as the %DET.

The surface EMG signals were also assessed using sample entropy (SampEn), a measure of signal complexity and regularity that has been derived specifically for physiological time-series signals (Richman and Moorman 2000). Briefly, SampEn quantifies the degree of uncertainty or randomness in the EMG signal using template matching, whereby a short epoch of the signal is defined as a template and that template is compared with the remainder of the signal to assess the conditional probability of it being repeated. A low value of entropy reflects a high degree of regularity in a signal (e.g. periodicity), with more similarity between each epoch of the signal. Sample entropy was calculated for each trial over the same period examined in the coherence analysis, SampEn was calculated over three 10 s windows with an overlap of 4.5 s during the constant force trials, and over two 10 s segments during the two-force trials (at the higher and

lower force levels, respectively). The tolerance *r* (threshold for similarity between templates) for the sample entropy calculation was given by Equation 3, where *MAD* is the median absolute deviation of the signal *x*.

$$r = k * MAD(x) \quad [6]$$

The embedding dimension (length of the template used for comparison) and parameter *k* were empirically set to 3 and 0.2, respectively (Flood et al. 2019). The tolerance scheme was selected based on each signal section under analysis to focus on the signal structure rather than its amplitude. The median value over all windows and channels in the 3rd dimension was used as the representative value for sample entropy.

Statistical analysis

All statistical analyses were performed in the software R (www.r-project.org, version 3.5.1). The relationship between beta-band coherence (and SampEn/Det) and the force of the muscle contraction (Force) was investigated with a linear mixed effects model with maximum likelihood fit using the lme4 library (Bates et al. 2012). A mixed effects model with unstructured variance covariance structure was used in order account for the statistical correlation between multiple coherence values obtained from the same subject, and to include the results of each trial in the statistical analysis without averaging. The coherence estimate obtained for each trial (first level) was nested according to Force (second level), which was in turn nested within each Subject (third level). Force was entered as a fixed effect in the model and Subject was included as a random effect, with a random intercept chosen for each subject to account for baseline differences in coherence. Previous simulation studies have shown that both the number of motor units used in the coherence calculation and the mean firing rate of these units can influence the estimated coherence (Farina et al. 2014; Lowery et al. 2007; McManus et al. 2016). The number of motor units used in the coherence calculation (MUnum) and the motor unit mean firing rate (MFR) for each trial were therefore used as predictor variables to assess their relative influence on the coherence estimate. A similar mixed model format was used to examine the effect of Force on the beta-band motor unit coherence during the two-force trials, with MFR and MUnum as predictor variables.

To examine whether motor unit coherence changed from the first to the second half of each trial, a mixed model was applied to the data, again incorporating predictor variables MFR and MUnum. An additional fixed effect was used to indicate whether the coherence estimate was obtained from the first or second half of the trial (Time) and an interaction term (Force*Time) was included in the model to investigate whether any change in coherence differed over the four

force levels. Lastly, motor unit coherence was estimated using the 8 largest and 8 smallest motor units for each trial, to assess whether there was any difference in the coherent activity of low- and high threshold motor units. Differences between the two populations were assessed using a mixed model with a fixed effect to indicate whether the coherence estimate was from a low- or high threshold motor unit subgroup (Group), in addition to MFR as a predictor variable. An interaction term (Force*Group) was included to examine whether any difference in coherence between the two populations varied over the four force levels. Model diagnostic plots were assessed to check for violations of regression assumptions, i.e., linearity, heteroscedasticity and normality (of both residuals and random effects). The variance inflation factor (VIF) of each predictor was calculated to ensure that there was no collinearity between the predictors (i.e. $VIF < 3$). The F-tests and p-values in the ANOVA table were generated using Kenward-Roger's method for denominator degrees-of-freedom and F. Differences in motor unit coherence and MFR across each force level were examined by pairwise comparisons of least-square means, using the Benjamini and Hochberg correction to account for multiple testing. Least-square means assesses the difference between force levels, while adjusting for the effect of any predictor variables included in the model (e.g. MUnum, MFR). The intra-class correlation coefficient (ICC) was calculated to report the proportion of variance in the motor unit coherence that could be explained by the grouping structure (i.e. variability due to inter-subject differences in baseline coherence). The conditional $R^2(c)$ and the marginal $R^2(m)$ were also estimated to determine the variance explained by the entire model (i.e. both fixed and random effects) and the variance of just the fixed effects, respectively (Nakagawa and Schielzeth 2013). To assess the relative importance of each fixed effect, semi-partial R^2 values were calculated for the effect of Force and for predictors (Edwards et al. 2008; Nakagawa and Schielzeth 2013).

To investigate the relationship between the motor unit coherence and the nonlinear features/force accuracy a repeated measures correlation analysis was performed for the constant force (N = 171 trials) and two-force trials (N = 142 trials, equivalent to 284 signal segments), as described by Bakdash and Marusich (2017). The relationship between beta-band coherence and the accuracy of the abduction force produced was further investigated with a linear mixed model, with the force level and beta-band coherence estimates included as possible predictors of force accuracy.

In figures depicting data pooled over all subjects, data were normalized per subject to focus on within-subject effects and minimize the contribution of inter-subject variance in baseline values to the visual representation of results. Data were normalized for a given subject by subtracting

353 that subject's mean coherence for the four force levels minus the grand mean of all subjects
354 (Loftus and Masson 1994).

355 Results

356 The relative effects of contraction force level, motor unit sample size and MU firing rate on
357 estimated motor unit beta-band coherence during constant force isometric contraction are first
358 presented. Motor unit coherence is also presented for trials where the same motor unit sample
359 was tracked across two force levels. The influence of the detected motor unit sample on the
360 coherence estimate is then further highlighted by examining differences in beta-band coherence
361 between low- and high threshold motor units. To investigate whether the development of fatigue
362 affected the coherence estimate at higher force levels, motor unit coherence during the first and
363 second half of the constant force contractions was compared. Finally, parallel changes in the
364 nonlinear surface EMG features are presented. The full mixed model results can be found in the
365 supplementary material http://dx.doi.org/10.5281/zenodo.3257376.

366 The average number of motor units detected during each trial is presented in Table 1, along with
367 the number of units that satisfied the acceptance criteria for further analysis. The mean
368 abduction force over all subjects was 23.6 ± 4.3N.

369 **Table 1**

370 Beta-band motor unit coherence decreased with increasing force during the constant force trials
371 between 10% and 40% MVC, Figure 1. The motor unit coherence spectrum and motor unit
372 mean firing rates are shown for a representative subject in Figure 2. The power spectra of the
373 individual single motor unit pulse trains featured a spectral peak at the mean discharge rate
374 (19.4 Hz and 11.8 Hz in Figure 3 (a)), and a smaller harmonic component at double the firing
375 frequency. The corresponding coherence spectrum shows a small, but significant peak at 30 Hz
376 that was not present in the power spectra, Figure 3 (a).The spectral peaks at ~10 Hz and ~30 Hz
377 were not clearly defined in coherence estimates from motor unit pairs, Figure 3 (a), but distinct
378 peaks emerged as more motor units were included in the estimation, Figure 3 (b) – (e). The
379 coherence between motor units disappeared when the estimate was obtained after shuffling the
380 interpulse intervals of the raw pulse trains, a process that removes any correlation between
381 motor unit discharges but maintains the same mean firing rates, Figure 3 (e). The maximum
382 number of available motor units was thus used to calculate the coherence estimate for each trial,
383 as various motor unit subsets could generate differing coherence spectra, Figure 3 (c) and (d).
384 Motor unit discharge times may be shifted by an oscillatory input, resulting in an increased
385 likelihood of a motor unit firing in response to the stimulus across the population.

A reduction in alpha-band motor unit coherence was also detected at higher force levels, however, a mixed model analysis indicated that a significant portion of the variance in the alpha-band coherence could be explained by differences in average motor unit firing rates. Higher motor unit mean firing rates resulted in lower alpha-band coherence estimates but firing rate had no effect on the beta-band, Table 2 and Table S1. Both the number of motor units used in the calculation (see also Figure 3) and the force level of the contraction influenced the coherence estimates. The mixed model enabled each trial to be included in the statistical analysis without averaging (N = 171 trials), allowing the inherent variability in coherence measurement to be explored and incorporated into all tests of significance. Approximately 40% (adjusted intraclass correlation coefficient, ICC = 0.4) of the total variance in motor unit coherence could be attributed to variance in the coherence estimate across subjects. Even with the inclusion of covariates and fixed factors, differences in subject baseline coherence could still account for over 20% of the variance in the motor unit coherence estimate (conditional ICC = 0.23).

Motor unit action potential amplitudes were larger at each consecutive force level ($F(3, 151) = 110.7$, $p < .001$), indicating the recruitment of larger motor units at higher force levels (10% MVC: 13.0 ± 7.5 μV), 20% MVC: 24.9 ± 12.1 μV, 30% MVC: 37.9 ± 20.2 μV, and 40% MVC: 48.2 ± 19.5 μV, $p < .001$ for all pairwise comparisons). Motor unit mean firing rates were also significantly affected by changing contraction force level ($F(3, 151) = 4.2$, $p = .007$), though pairwise comparisons only revealed a significant difference between mean firing rates at 10% MVC (14.7 ± 2.7 Hz) and both 30% MVC (13.6 ± 2.4 Hz, $p = .017$) and 40% MVC (13.7 ± 1.8 Hz, $p = .015$), and not between 10 % and 20% MVC (14.0 ± 2.5 Hz, $p = .099$). Together, these results suggest the recruitment of larger, higher threshold motor units with lower mean firing rates as force was increased (McManus et al. 2015).

Figure 1

Figure 2

Figure 3

Force level had a significant effect on beta-band motor unit coherence during the constant force trials (semi-partial $R^2 = 0.19$ and 0.22, respectively), Table 2 (a), and had an even greater influence on coherence during the two-force trials, where the coherence estimate was calculated on the same sample of motor units across two different force levels (semi-partial $R^2 = 0.29$ and 0.31, respectively), Table 2 (b) and Figure 4. The decrease/increase in coherence as force was increased/decreased was even more pronounced when analyzing the same motor unit sample

419 across force levels, Figure 4 (a) and (b), respectively. Though alpha-band coherence exhibited
420 similar changes to those observed in the beta-band, a significant proportion of the variation in
421 alpha-band coherence was again explained by differences in motor unit MFR, with no influence
422 of MFR on beta-band coherence detected, Table S1.

423 Consistent with the constant force isometric contractions, contraction force also affected motor
424 unit mean firing rates during the two-force trials ($F(7, 260) = 5.8$, $p < .001$). Motor unit mean
425 firing rates, estimated from a constant MU population, were significantly altered when the force
426 was decreased from 20→ 10% MVC (14.1 ± 2.8 Hz to 12.9 ± 2.5 Hz, $p = .01$) and when force
427 was increased from 10→ 20% MVC (13.6 ± 2.5 Hz to 14.5 ± 2.6 Hz, $p = .047$). When the motor
428 unit firing rates during the two-force trials were compared with those recorded during the
429 constant force trials, firing rates were higher when force was increased to 30% MVC (14.1 ± 2.2
430 Hz, $p = .019$) from 20% MVC when compared with the constant force trial at 30% MVC,
431 Figure 4 (c). Similarly, motor unit mean firing rates were lower when the contraction force was
432 decreased from 30% to 20% MVC ($p = .027$) and from 20% to 10% MVC ($p < .001$), when
433 compared with the trials at a single constant force, Figure 4 (c).

434 **Table 2**

435 **Figure 4**

436 When the beta-band coherence estimate was compared between groups of low- and high
437 threshold motor units, it was consistently greater in larger, high threshold motor units ($F(1, 287)$
438 $= 23.38$, $p < .001$), Table S2. Beta-band coherence was larger in high threshold motor units at
439 all force levels, while accounting for increases in the coherence estimate that could be attributed
440 to lower mean firing rates. The difference in beta-band coherence between low- and high
441 threshold motor units is shown for 40% MVC across all subjects in Figure 5 (a) and for a single
442 trial at 20% MVC in a respresentative subject in Figure 5 (b). Though differences between
443 motor unit groups did not vary across the four force levels for the beta-band coherence ($F(3,$
444 $274) = 1.37$, $p = .25$), a significant interaction between Force*Group was detected in the alpha-
445 band coherence ($F(3, 273) = 2.98$, $p = .03$). Alpha-band coherence estimates differed between
446 low- and high threshold motor units in the 10 and 20% MVC trials ($p < .0001$ and $p = .004$,
447 respectively), but not for the trials at 30 and 40% MVC ($p = .09$ and $p = .39$, respectively), when
448 differences in motor unit MFR were considered.

449 **Figure 5**

450 Motor unit coherence during the constant force trials was then compared between the first and
451 second half of the contraction, with beta-band coherence shown in Figure 6 (a). Motor unit

coherence was significantly higher during the second half of the trial in both the alpha- and beta-band ($F(1, 316) = 19.86$, $p < .001$ and $F(1, 316) = 21.0$, $p < .001$, respectively), Table S3. The progressive increase in the beta-band coherence during the contraction is shown for a representive subject at 30% MVC in Figure 6 (c). This was accompanied by a decrease in the median frequency of the surface EMG signal during the sustained contraction at 20%, 30% and 40% MVC, Figure 6 (b), indicating the development of peripheral fatigue, associated with reduced muscle fiber conduction velocity as the contraction progressed at higher force levels. The increase in coherence from the first to the second half of the trials did not vary across the four force levels in the alpha-band ($F(3, 316) = 1.35$, $p = .26$). However, alterations in beta-band coherence differed according to force level ($F(3, 316) = 4.21$, $p = .006$), with a significant increase detected at the higher force levels 30% and 40% MVC ($p = .008$ and $p < .001$, respectively) but no change observed at 10% and 20% MVC ($p = .92$ and $p = .27$, respectively). Motor unit mean firing rates influenced both the alpha- and beta-band coherence estimate ($F(3, 279) = 52.15$, $p < .001$ and $F(1, 294) = 5.55$, $p = .019$, respectively), however, this effect was stronger in the alpha-band estimates when compared with the beta-band (semi-partial $R^2 = 0.19$ and 0.02, respectively).

Figure 6

Cross-correlogram analysis revealed the presence of a peak (of varying amplitude) centered around zero lag in approximately 58 ± 10% of motor unit pairs, indicating an excess of co-incident firing between two motor units, Figure 7 (A). A relatively small number of motor unit pairs (5 ± 4%) exhibited a dip or “trough” at zero lag, Figure 7 (A). It was found that troughs similar to those detected in experimental data could be artificially induced in the cross-correlogram of motor unit pairs by removing co-incident firing instances from one of the motor units in the pair, Figure 7 (C). Shifting co-incident firings (by 3 ms or less) in one motor unit relative to the other motor unit created a wider peak in the cross-correlogram, Figure 7 (C). Figure 7 (C) illustrates the effect that such errors in the precise timing of motor unit firing instances could have on the cross-correlogram. The results of the cross-correlogram analysis suggest that missed coincident firings did not significantly influence the observed reduction in motor unit coherence at higher force levels. First, there was no systematic change in the percentage of motor unit pairs that exhibited troughs at zero in the cross-correlogram, which indicates that the number of missed coincident firings did not increase at higher force levels ($F(3, 151) = 0.49$, $p = .69$, Figure 7 (B) . There was, however, a significant decrease in the detection of significant peaks ($F(3, 152) = 5.2$, $p = .002$), consistent with the reduction in beta-band coherence. Second, a decrease in both alpha and beta-band coherence remained following

the removal of motor units that were identified as having high levels of missed co-incident firings ($F(3, 143) = 24.5$, $p < .001$ and $F(3, 142) = 33.12$, $p < .001$, respectively). In addition, higher threshold motor units still exhibited greater alpha- and beta-band coherence than lower threshold units ($F(1, 303) = 30.6$, $p < .001$ and $F(1, 283) = 5.5$, $p = .02$, respectively). There was no difference in the number of motor units removed at each force level (average of 1.4 ± 2.3 motor units per trial, $F(3, 143) = 0.5$, $p = .68$). Lastly, artificially introducing missed co-incident firings into 10% of the total number of motor unit pairs in experimental data did not have a large effect on the coherence spectrum, Figure 7 (D).

Figure 7

The nonlinear features extracted from the surface EMG signal exhibited comparable changes to those observed in the underlying motor unit coherence. During the constant force contractions, the %DET of the surface EMG signal decreased, and the SampEn showed a corresponding increase, Figure 8 (a) and (b), respectively, indicating an increase in the surface EMG complexity. The changes in the nonlinear features during the two-force trials also mirrored the decrease in coherence observed as force was increased, Figure 8 (c), and reciprocal increase as force was decreased, Figure 8 (d). An increase in %DET was detected during the second half of the contraction at higher force levels, Figure 6 (b), mirroring the observed increase in beta-band motor unit coherence, and the inverse trend was found in the sample entropy. SampEn and %DET were more sensitive than motor unit coherence to inter-subject differences, which could account for ~70% of the variance in these measures (conditional ICC = 0.76 and 0.62, respectively). The nonlinear parameters were weakly correlated with beta- and alpha-band motor unit coherence obtained during the constant force level trials, Table 3. A stronger correlation was observed between the nonlinear parameters and coherence during the two-force trials, Table 3, where more pronounced changes in motor unit coherence were observed, Figure 4.

Beta-band motor unit coherence exhibited a significant correlation with the root mean square error ($r = -0.34$ [-0.47 -0.19], $p < .001$) and the coefficient of variation of the index finger abduction force ($r = 0.22$ [0.07 0.36], $p = .005$). However, the results of the mixed model analysis indicate that differences in level of beta-band coherence across trials were unable to account for any additional variability in force accuracy, after changes in force level were considered. The RMSE of the force produced increased at higher force levels ($F(3, 152) = 64.3$, $p < .001$) and the beta-band coherence estimate was not a significant predictor of variability in force accuracy ($F(1, 165) = 0.008$, $p = .92$). Conversely, the force coefficient of variation decreased at higher force levels ($F(3, 153) = 8.4$, $p < .001$), but again beta-band coherence did

not have a significant effect on the variation independent of changes in force level ($F(1, 164) = 0.17$, $p = .68$).

Table 3

Figure 8

Discussion

The present study shows for the first time a progressive reduction in beta-band intramuscular coherence as muscle force increases during index finger abduction, Figure 1 and Figure 4. During the 10% MVC contractions, two peaks were generally observed in the coherence spectrum at 10-15 Hz and 25-35 Hz (similar to the peaks observed in pooled coherence between motor unit pairs (Halliday et al. 1999; Semmler et al. 2003)). The beta-band peak between 25-35 Hz was more commonly detected at the lower force levels and was often absent or replaced by broad-band coherence at the higher contraction intensities. Coherent beta-band motor unit activity is widely believed to be cortical in origin, arising as a result of synchronized pre-synaptic inputs to the motoneuron pool (Baker et al. 2003). Such inputs would alter the firing probability of motor units, Figure 3 (f), introducing a correlation between motor unit firing trains at the frequency of the shared oscillatory modulation. This component is not present between motor units discharging independently regardless of any similarity in mean firing rates, Figure 3 (e). Motor unit mean firing rates can, however, influence the expression of coherent activity in the motor unit discharges. Most motor units detected in the current study discharged at rates below 20-35 Hz and would thus only respond intermittently to an external modulation in this frequency range. A relatively large motor unit sample may therefore be necessary to effectively capture the collective beta-band modulation, Figure 3. An oscillatory input to the motoneuron pool is likely to induce synchronous firings in different combinations of motor units over the course of the muscle contraction. The inclusion of multiple simultaneously active motor units in the composite pulse trains will therefore increase the effective sampling of this modulation at any given point in time and is likely to enhance the detection of coherent activity when compared with alternative methods such as pooled coherence from paired motor unit recordings. The results suggest that the accurate estimation of beta-band coherence using composite pulse trains requires a larger number than the 5 MU minimum proposed for examining coherence at lower frequencies (Farina et al. 2014). Accordingly, in the present study, coherence estimates were likely to be greater when more motor units were included in the calculation, Table 2. An inhomogeneous distribution of coherent activity across the motor unit population could also contribute to this effect, if more high threshold motor units were present in the detected motor unit sample, Figure 5. Changes in motor unit coherence in the present study were thus assessed while aiming to control for some of the variability introduced by using different numbers of motor units for each coherence calculation (MUnum), Table 2. In studies investigating changes in motor unit coherence across conditions, this approach may be preferable to restricting the number of motor units used in the coherence calculation to a constant number across trials, as coherence could vary substantially based on the randomly

559 chosen motor unit sample, Figure 3 (c) and (d). A large portion of the variability in the
560 coherence estimates could be attributed to motor unit sample size and inter-subject differences
561 in baseline coherence (ICC, 20-40%), however, neither of these factors could account for the
562 decrease in motor unit coherence observed with increasing force.

563 A decrease in alpha-band coherence was also observed alongside the reduction in beta-band
564 coherence but estimates in this frequency range were disparately affected by variations in motor
565 unit mean firing rate and contraction force level. Though previous studies in humans and
566 primates have provided evidence that the ~10 Hz modulation of motor unit discharges during
567 isometric contractions is cortical or sub-cortical in origin (Marsden et al. 2001; Williams et al.
568 2009), the alpha-band component is also influenced by muscle spindle activity and resonance
569 within the afferent feedback loops (Christakos et al. 2006; McManus et al. 2013). The
570 generation of motor unit synchrony in the alpha-band range is thus likely multifactorial, and the
571 results of the present study indicate that the average motor unit firing rate is another
572 contributing component. Higher motor unit mean firing rates were associated with lower alpha-
573 band coherence estimates, Table 2. This suggests that motor units are more powerfully entrained
574 by ~10 Hz central oscillators and/or peripheral feedback loop resonances when their average
575 firing rates lie closer to this frequency (see Figure 5 (a) in Lowery et al. (2007)). The average
576 firing rate in each trial did not significantly influence the beta-band coherence estimate.
577 However, it is likely that the average discharge rate estimated over all motor units does not fully
578 capture the complex interaction between motoneuron firing rate and its responsiveness to a
579 synchronizing input. Changes in average motoneuron firing rates could alter the resulting
580 expression of coherence or synchronization in the motor unit discharges and influence how
581 effectively synaptic inputs can be detected (Kline and De Luca 2015; Lowery and Erim 2005).

582 The observed decrease in motor unit coherence with increasing force mirrors the reduction in
583 beta-band corticomuscular coherence reported for the FDI muscle during index finger abduction
584 within a similar force range (Perez et al. 2012). It is thus possible that the change in beta-band
585 coherence reflects a collective decrease in coherent beta-band activity within the motor cortex
586 with increasing contraction strength. It has been shown that beta-band oscillations are stronger
587 in the presence of higher intracortical inhibition (Matsuya et al. 2017), which is progressively
588 suppressed as the strength of a muscle contraction increases (Zoghi and Nordstrom 2007). There
589 is also experimental evidence to suggest that cortical beta-band oscillations are reduced during
590 periods of increased neuronal firing rates during brief muscle contractions (<1 s) (Ritter et al.
591 2009; Spinks et al. 2008), however, this may not extend to longer duration contractions and it is

592 also unclear whether beta-band activity in the motor cortex is modulated with force (Dal Maso
593 et al. 2017; Mima and Hallett 1999).

594 Alternatively, it is possible that an increase in other inhibitory or excitatory inputs to the
595 motoneuron pool could dilute or diminish the relative strength of the synchronized input. If the
596 level of asynchronous inputs increases, the efficacy of a synchronous oscillatory input at
597 inducing coherent motor unit firing will be reduced. Though the corticospinal system has a
598 prominent role in the production of weak forces in tasks requiring fine, fractionated control of
599 finger muscles (Laurence and Kuypers 1968), stronger forces may require excitatory inputs
600 from other descending pathways. In particular, there is evidence to suggest that contributions
601 from the reticulospinal pathway become increasingly important during stronger muscle
602 contractions in intrinsic hand muscles (Baker 2011). Changes in excitation from descending
603 pathways may also influence motoneurons indirectly through local segmental interneurons
604 (Alstermark and Isa 2012). Changes in either descending (Cheney et al. 1991; Riddle et al.
605 2009) or afferent information (Hultborn and Pierrot-Deseilligny 1979; Macefield et al. 1996;
606 Pierrot-Deseilligny and Burke 2005) at higher muscle forces could generate complex
607 interactions within interneuronal networks, altering their effects on the motoneuron population.
608 Afferent activity could also indirectly influence coherent motor unit firing via supraspinal
609 centers as part of a beta-synchronized feedback loop (Baker et al. 2006; Witham et al. 2007).
610 Experimental evidence indicates that beta-range corticomuscular and intermuscular coupling
611 can be modulated by ascending sensory pathways (Fisher et al. 2002; Kilner et al. 2004; Pohja
612 and Salenius 2003). Consequently, alterations in either afferent and efferent activity could
613 disrupt the bidirectional flow of information that exists between oscillatory beta-band cortical
614 and muscular activities (Witham et al. 2011).

615 Finally, a decrease in motoneuron responsiveness to an oscillatory input could also arise from
616 increases in background synaptic noise, which can vary with motoneuron background discharge
617 rates (see review by Powers and Türker (2010)). At higher motoneuron firing rates, increases in
618 membrane conductance reduce the synaptic current reaching the soma from the dendritic
619 synapses, lowering the spike-triggering efficacy of an excitatory postsynaptic potential input. It
620 is possible that an increase in the activity of persistent inward currents in the motoneuron could
621 similarly contribute to a decrease in motor unit coherence (Taylor and Enoka 2004), but this has
622 yet to be systematically explored (Powers and Türker 2010). Lastly, it should be noted that none
623 of the above-mentioned hypotheses are mutually exclusive. All factors could potentially
624 contribute to a reduction in coherence at higher force levels, though it is not possible to draw
625 definitive conclusions on the underlying mechanisms based on the data presented. Additionally,

626 changes in motor unit coherence with increasing force are likely to be muscle and task
627 dependent, as the relative contribution of various descending pathways will differ across
628 muscles and movements. The decrease in motor unit coherence at higher force levels could be
629 specific to muscles involved in fine motor control, and may not be observed in larger muscles
630 (Laine et al. 2015). Tasks that require the co-ordination of several muscles may also yield
631 different results, though the contribution from muscles other than the FDI is likely to be
632 minimal during index finger abduction (Infantolino and Challis 2010).

633 Due to the nature of surface EMG decomposition there is a higher likelihood of a motor unit
634 firing being missed when two motor units discharge within a few milliseconds of one another,
635 when compared with intramuscularly recorded motor units. However, the results suggest that
636 missed co-incident firings do not account for the observed reduction in motor unit coherence
637 with increasing force, as there was no systematic increase in the number of missed firings at
638 higher force levels (which could contribute to the observed reduction in motor unit coherence),
639 Figure 7 (B). Furthermore, when motor units with high levels of missed firings were removed
640 from the analysis, the decrease in coherence remained. The results of the current study also
641 present evidence that motor unit coherence is less sensitive than synchronization measures to
642 the firing time accuracy in motor units, Figure 7 (D), and provides a more global measure of
643 population synchrony. The results highlight the importance of reporting time-domain data
644 alongside coherence analysis when presenting results based on motor unit firing trains from
645 decomposed surface EMG.

646 *Differences in beta-band coherence between high- and low threshold MUs*

647 Beta-band coherence was consistently larger in high threshold motor units, Figure 5. This
648 complements the results of previous studies that have found greater short-term synchronization
649 between high threshold motor unit pairs (Datta and Stephens 1990; Schmied et al. 2014). High
650 threshold motor units, but not low threshold units, also exhibited increased coherent beta-band
651 activity when execution errors were amplified during a force tracking task (Hwang et al. 2017).
652 Large EPSPs may be more likely to trigger an action potential in motoneurons firing at low,
653 'subprimary' firing rates (Matthews 1996), as the membrane voltage lies in a plateau phase
654 close to the firing threshold for a larger proportion of the interspike interval (Powers and Türker
655 2010). While firing rate differences may contribute to the difference in coherence between high-
656 and low threshold units, Figure 5, there is also experimental evidence to suggest that
657 corticospinal inputs are greater in high threshold motoneurons in decerebrate cats (Binder et al.
658 1998) and primates (Clough et al. 1968). Alpha-band coherence also differed between high- and

low threshold motor units. However, a significant difference was only detected for the 10% and 20%MVC trials, after variations in motor unit mean firing rates were accounted for.

Variations in beta-band coherence from the start to the end of the contraction

During the trials performed at a constant force, beta-band motor unit coherence increased during the second half of the 30% and 40% MVC contractions, Figure 6 (a), accompanied by a decrease in the surface EMG median frequency, Figure 6 (b). In contrast, alpha-band coherence showed a consistent increase during the second half of the trial at all force levels. The indication of peripheral fatigue as the contraction progressed suggests that the parallel increase in beta-band coherence at higher forces also occurred a result of fatigue. A progressive increase in motor unit synchronization, alpha- and beta-band coherence during a fatiguing contraction, and directly post-fatigue, has been previously demonstrated within the FDI muscle (Kattla and Lowery 2010; McManus et al. 2016). Parallel changes in the EMG signal structure were also observed, Figure 6 (b), providing further evidence that these features are influenced by muscular fatigue (Cashaback et al. 2013; Farina et al. 2002; Webber et al. 1995).

Changes in beta-band coherence during the two-force trials

The effect of contraction strength on beta-band coherence was much more pronounced in the trials where the same motor units were tracked over two force levels, Figure 4. When abduction force was increased or decreased during the second half of the trial the beta-band coherence decreased or increased, respectively. As the coherence estimate was calculated over a shorter time period (10 s vs 23 s), with fewer motor units (approximately 20% less, Table 1), the coherence values during the first half of the two-force trials were lower than those reported for the same contraction strength during the constant force trials. High threshold motor units that were recruited/de-recruited during the contraction were excluded from the analysis. It is also possible that small, low threshold motor units were more likely to be missed in the two-force trials as a result of the transition to/from higher force levels. Though a smaller subset of motor units may have been detected during the two-force trials, average MU firing rates during the first half of the ramp trials were comparable to those reported during the constant force trials, Figure 4 (c). However, during the decreasing force trials, average firing rates during the second half of the two-force trial were significantly lower than for the corresponding constant force trials. Conversely, during the increasing force trials from 20 → 30 % MVC, motor units tended to fire faster at the higher force level when compared with the equivalent constant force trials. The higher or lower motor unit mean firing rates during the second half of the ramp trials may be a response to muscle force depression or enhancement that can occur following active muscle

shortening or lengthening, respectively (Herzog 2004). Prior shortening of a muscle has been shown to require greater neural activation to maintain a given isometric force, and conversely, lower surface EMG amplitudes have been observed following lengthening contractions (Jones et al. 2016). In the present study, lower MU firing rates at 20% MVC and 10% MVC were accompanied by higher beta-band coherence in contractions that were preceded by a decrease in abduction force, Figure 4 (b). A similar difference was observed in the nonlinear surface EMG features, Figure 8 (d). Conversely, beta-band coherence was lower at 20% MVC when the contraction was preceded by an increase in force, Figure 3 (a).

Relationship between motor unit coherence and the Nonlinear Parameters and Force Accuracy

The changes in motor unit coherence presented in the current study were supported by corresponding changes in nonlinear parameters calculated from the surface EMG signal, Figure 8. A secondary result of this study was the novel detection of a significant, moderate correlation between nonlinear features based on the surface EMG signal (%DET and SampEn) and the underlying motor unit coherence, Table 3. The estimation of coherence across the motoneuron pool and the inclusion of a greater range of contraction forces may have facilitated the detection of a relationship between these two measures, as this type of protocol and data analysis were not previously possible with intramuscular EMG (Dideriksen et al. 2009; Schmied and Descarreaux 2011). In the present study %DET decreased with increasing force, exhibiting the same trends as the beta-band motor unit coherence, Figure 8 (b). SampEn, a measure approximately inversely related to %DET, increased with increasing contraction strength, Figure 8 (a). Previous studies using various entropy measures have found similar increases with increasing force (Cashaback et al. 2013; Kaplanis et al. 2010), though reports on the sensitivity of %DET and SampEn to changes in muscle contraction level vary (Del Santo et al. 2007; Meigal et al. 2009). A stronger relationship between the coherence and the nonlinear features was detected for the two-force trials, where changes in coherence were more pronounced, than for trials at a constant force level, Table 3, Figure 4 (a) and (b). However, it is important to note that motor unit coherence is unlikely to be the only factor contributing to the observed changes in the nonlinear features, as increases in surface EMG signal density due to increased motor unit recruitment and firing rate could also alter the SampEn and %DET. Collectively, the results suggest that SampEn and %DET could be useful in detecting large differences in motor unit coherence, i.e. during muscular fatigue (Cashaback et al. 2013; Farina et al. 2002; Webber et al. 1995) or in pathological conditions (Fattorini et al. 2005; Flood et al. 2019; Meigal et al. 2009). The results also highlight the sensitivity of these features to inter-subject differences in

726 physiology (e.g. muscle size, motor unit distribution), and the need to consider muscle
727 contraction strength in any quantitative analysis.

728 Finally, variations in the force accuracy of trials performed at the same force could not be
729 explained by differences in beta-band motor unit coherence, though coherence was correlated
730 with force accuracy across different force levels. Studies investigating corticomuscular
731 coherence have reported that motor performance was not associated with the level of beta-band
732 coherence during index finger abduction and ankle dorsi-plantarflexion (Johnson et al. 2011;
733 Perez et al. 2006). Other studies employing isometric force compensation protocols have found
734 that higher beta-band corticomuscular coherence was associated with decrease relative error in
735 force (Kristeva et al. 2007; Witte et al. 2007), possibly reflecting a higher contribution from
736 afferent sensory feedback during this type of task (Lim et al. 2014).

737 In conclusion, a reduction in beta-band intramuscular coherence was observed with increasing
738 muscle force. The variations in coherence during changes in muscle activation level and with
739 the onset of fatigue were accompanied by parallel changes in the SampEn and %DET of the
740 surface EMG signal, and a significant relationship between the nonlinear features and the
741 underlying motor unit coherence was demonstrated for the first time. The results show that the
742 properties of the detected motor unit sample and level of activation of the muscle are important
743 factors to consider when investigating the modulation or disruption of beta-band activity.

Additional Information

Competing interests: No conflicts of interest, financial or otherwise, are declared by the authors.

Acknowledgements: We would like to thank Mr Jérémy Liegey for help with experimental work.

References

Alstermark B, and Isa T. Circuits for skilled reaching and grasping. *Annual review of neuroscience* 35: 559-578, 2012.

Bakdash JZ, and Marusich LR. Repeated measures correlation. *Frontiers in psychology* 8: 456, 2017.

Baker SN. The primate reticulospinal tract, hand function and functional recovery. *The Journal of physiology* 589: 5603-5612, 2011.

Baker SN, Chiu M, and Fetz EE. Afferent encoding of central oscillations in the monkey arm. *Journal of neurophysiology* 95: 3904-3910, 2006.

Baker SN, Pinches EM, and Lemon RN. Synchronization in monkey motor cortex during a precision grip task. II. Effect of oscillatory activity on corticospinal output. *Journal of neurophysiology* 89: 1941-1953, 2003.

Bates D, Maechler M, and Bolker B. lme4: linear mixed-effects models using S4 classes. R package version 0.999375-42. 2011. *Google Scholar* 2012.

Binder MD, Robinson FR, and Powers RK. Distribution of effective synaptic currents in cat triceps surae motoneurons. VI. Contralateral pyramidal tract. *Journal of neurophysiology* 80: 241-248, 1998.

Cashaback JG, Cluff T, and Potvin JR. Muscle fatigue and contraction intensity modulates the complexity of surface electromyography. *Journal of Electromyography and Kinesiology* 23: 78-83, 2013.

Castronovo AM, Negro F, Conforto S, and Farina D. The proportion of common synaptic input to motor neurons increases with an increase in net excitatory input. *Journal of Applied Physiology* jap. 00255.02015, 2015.

Cheney PD, Fetz EE, and Mewes K. Neural mechanisms underlying corticospinal and rubrospinal control of limb movements. In: *Progress in brain research*Elsevier, 1991, p. 213-252.

Christakos CN, Papadimitriou NA, and Erimaki S. Parallel neuronal mechanisms underlying physiological force tremor in steady muscle contractions of humans. *Journal of neurophysiology* 95: 53-66, 2006.

Christou EA, Rudroff T, Enoka JA, Meyer F, and Enoka RM. Discharge rate during low-force isometric contractions influences motor unit coherence below 15 Hz but not motor unit synchronization. *Experimental brain research* 178: 285-295, 2007.

Clough J, Kernell D, and Phillips C. The distribution of monosynaptic excitation from the pyramidal tract and from primary spindle afferents to motoneurones of the baboon's hand and forearm. *The Journal of physiology* 198: 145-166, 1968.

Conway B, Halliday D, Farmer S, Shahani U, Maas P, Weir A, and Rosenberg J. Synchronization between motor cortex and spinal motoneuronal pool during the performance of a maintained motor task in man. *The Journal of physiology* 489: 917-924, 1995.

Dal Maso F, Longcamp M, Cremoux S, and Amarantini D. Effect of training status on beta-range corticomuscular coherence in agonist vs. antagonist muscles during isometric knee contractions. *Experimental brain research* 235: 3023-3031, 2017.

Datta A, and Stephens J. Synchronization of motor unit activity during voluntary contraction in man. *The Journal of physiology* 422: 397-419, 1990.

Del Santo F, Gelli F, Ginanneschi F, Popa T, and Rossi A. Relation between isometric muscle force and surface EMG in intrinsic hand muscles as function of the arm geometry. *Brain research* 1163: 79-85, 2007.

Dideriksen JL, Falla D, Baekgaard M, Mogensen ML, Steimle KL, and Farina D. Comparison between the degree of motor unit short-term synchronization and recurrence quantification

analysis of the surface EMG in two human muscles. *Clinical neurophysiology* 120: 2086-2092, 2009.
Edwards LJ, Muller KE, Wolfinger RD, Qaqish BF, and Schabenberger O. An R2 statistic for fixed effects in the linear mixed model. *Statistics in medicine* 27: 6137-6157, 2008.
Elble RJ, and Randall JE. Motor-unit activity responsible for 8-to 12-Hz component of human physiological finger tremor. *Journal of neurophysiology* 39: 370-383, 1976.
Enochson LD, and Goodman NR. Gaussian approximations to the distribution of sample coherence MEASUREMENT ANALYSIS CORP LOS ANGELES CA, 1965.
Farina D, Fattorini L, Felici F, and Filligoi G. Nonlinear surface EMG analysis to detect changes of motor unit conduction velocity and synchronization. *Journal of Applied Physiology* 93: 1753-1763, 2002.
Farina D, Negro F, and Dideriksen JL. The effective neural drive to muscles is the common synaptic input to motor neurons. *The Journal of physiology* 592: 3427-3441, 2014.
Farmer S, Bremner F, Halliday D, Rosenberg J, and Stephens J. The frequency content of common synaptic inputs to motoneurones studied during voluntary isometric contraction in man. *The Journal of physiology* 470: 127-155, 1993.
Fattorini L, Felici F, Filligoi G, Traballesi M, and Farina D. Influence of high motor unit synchronization levels on non-linear and spectral variables of the surface EMG. *Journal of neuroscience methods* 143: 133-139, 2005.
Fisher R, Galea M, Brown P, and Lemon R. Digital nerve anaesthesia decreases EMG-EMG coherence in a human precision grip task. *Experimental brain research* 145: 207-214, 2002.
Fling BW, Christie A, and Kamen G. Motor unit synchronization in FDI and biceps brachii muscles of strength-trained males. *Journal of Electromyography and Kinesiology* 19: 800-809, 2009.
Flood MW, Jensen BR, Malling A-S, and Lowery MM. Increased EMG intermuscular coherence and reduced signal complexity in Parkinson's disease. *Clinical neurophysiology* 130: 259-269, 2019.
Gallet C, and Julien C. The significance threshold for coherence when using the Welch's periodogram method: effect of overlapping segments. *Biomedical Signal Processing and Control* 6: 405-409, 2011.
Halliday D, and Rosenberg J. On the application, estimation and interpretation of coherence and pooled coherence. *Journal of neuroscience methods* 100: 173-174, 2000.
Halliday DM, Conway BA, Farmer SF, and Rosenberg JR. Load-independent contributions from motor-unit synchronization to human physiological tremor. *Journal of neurophysiology* 82: 664-675, 1999.
Herzog W. History dependence of skeletal muscle force production: Implications for movement control. *Human movement science* 23: 591-604, 2004.
Hu X, Rymer WZ, and Suresh NL. Reliability of spike triggered averaging of the surface electromyogram for motor unit action potential estimation. *Muscle & nerve* 48: 557-570, 2013.
Hultborn H, and Pierrot-Deseilligny E. Changes in recurrent inhibition during voluntary soleus contractions in man studied by an H-reflex technique. *The Journal of physiology* 297: 229-251, 1979.
Hwang S, Lin Y-T, Huang W-M, Yang Z-R, Hu C-L, and Chen Y-C. Alterations in neural control of constant isometric contraction with the size of error feedback. *PLoS ONE* 12: e0170824, 2017.
Infantolino BW, and Challis JH. Architectural properties of the first dorsal interosseous muscle. *Journal of anatomy* 216: 463-469, 2010.
Johnson AN, Wheaton LA, and Shinohara M. Attenuation of corticomuscular coherence with additional motor or non-motor task. *Clinical neurophysiology* 122: 356-363, 2011.

844 **Jones AA, Power GA, and Herzog W**. History dependence of the electromyogram: Implications
845 for isometric steady-state EMG parameters following a lengthening or shortening contraction.
846 *Journal of Electromyography and Kinesiology* 27: 30-38, 2016.
847 **Kaplanis PA, Pattichis CS, and Zazula D**. Multiscale entropy-based approach to automated
848 surface EMG classification of neuromuscular disorders. *Medical & biological engineering &*
849 *computing* 48: 773-781, 2010.
850 **Kattla S, and Lowery MM**. Fatigue related changes in electromyographic coherence between
851 synergistic hand muscles. *Experimental brain research* 202: 89-99, 2010.
852 **Kilner JM, Baker SN, Salenius S, Hari R, and Lemon RN**. Human cortical muscle coherence is
853 directly related to specific motor parameters. *Journal of neuroscience* 20: 8838-8845, 2000.
854 **Kilner JM, Fisher RJ, and Lemon RN**. Coupling of oscillatory activity between muscles is
855 strikingly reduced in a deafferented subject compared with normal controls. *Journal of*
856 *neurophysiology* 92: 790-796, 2004.
857 **Kirkwood PA**. The origin of motoneuron synchronization. *Journal of neurophysiology* 115:
858 1077-1078, 2016.
859 **Kline JC, and De Luca CJ**. Synchronization of Motor Unit Firings: An Epiphenomenon of Firing
860 Rate Characteristics Not Common Inputs. *Journal of neurophysiology* jn. 00452.02015, 2015.
861 **Kristeva R, Patino L, and Omlor W**. Beta-range cortical motor spectral power and
862 corticomuscular coherence as a mechanism for effective corticospinal interaction during
863 steady-state motor output. *Neuroimage* 36: 785-792, 2007.
864 **Laine CM, Martinez-Valdes E, Falla D, Mayer F, and Farina D**. Motor neuron pools of
865 synergistic thigh muscles share most of their synaptic input. *Journal of neuroscience* 35: 12207-
866 12216, 2015.
867 **Laurence D, and Kuypers H**. The functional organization of the motor system in the monkey. II.
868 The effects of lesions of the descending brain-stem pathways. *Brain* 91: 15-36, 1968.
869 **Lim M, Kim JS, Kim M, and Chung CK**. Ascending beta oscillation from finger muscle to
870 sensorimotor cortex contributes to enhanced steady-state isometric contraction in humans.
871 *Clinical neurophysiology* 125: 2036-2045, 2014.
872 **Loftus GR, and Masson ME**. Using confidence intervals in within-subject designs. *Psychonomic*
873 *bulletin & review* 1: 476-490, 1994.
874 **Lowery MM, and Erim Z**. A simulation study to examine the effect of common motoneuron
875 inputs on correlated patterns of motor unit discharge. *Journal of computational neuroscience*
876 19: 107-124, 2005.
877 **Lowery MM, Myers LJ, and Erim Z**. Coherence between motor unit discharges in response to
878 shared neural inputs. *Journal of neuroscience methods* 163: 384-391, 2007.
879 **Macefield VG, Häger-Ross C, and Johansson RS**. Control of grip force during restraint of an
880 object held between finger and thumb: responses of cutaneous afferents from the digits.
881 *Experimental brain research* 108: 155-171, 1996.
882 **Marsden JF, Brown P, and Salenius S**. Involvement of the sensorimotor cortex in physiological
883 force and action tremor. *Neuroreport* 12: 1937-1941, 2001.
884 **Marwan N, Romano MC, Thiel M, and Kurths J**. Recurrence plots for the analysis of complex
885 systems. *Physics reports* 438: 237-329, 2007.
886 **Matsuya R, Ushiyama J, and Ushiba J**. Inhibitory interneuron circuits at cortical and spinal
887 levels are associated with individual differences in corticomuscular coherence during isometric
888 voluntary contraction. *Scientific reports* 7: 44417, 2017.
889 **Matthews P**. Relationship of firing intervals of human motor units to the trajectory of post-
890 spike after-hyperpolarization and synaptic noise. *The Journal of physiology* 492: 597-628, 1996.
891 **McAuley J, and Marsden C**. Physiological and pathological tremors and rhythmic central motor
892 control. *Brain* 123: 1545-1567, 2000.

McManus L, Hu X, Rymer WZ, Lowery MM, and Suresh NL. Changes in motor unit behavior following isometric fatigue of the first dorsal interosseous muscle. *Journal of neurophysiology* 113: 3186-3196, 2015.

McManus L, Hu X, Rymer WZ, Suresh NL, and Lowery MM. Muscle fatigue increases beta-band coherence between the firing times of simultaneously active motor units in the first dorsal interosseous muscle. *Journal of neurophysiology* 115: 2830-2839, 2016.

McManus LM, Budini F, Di Russo F, Berchicci M, Menotti F, Macaluso A, De Vito G, and Lowery MM. Analysis of the effects of mechanically induced tremor on EEG-EMG coherence using wavelet and partial directed coherence. In: *Neural Engineering (NER), 2013 6th International IEEE/EMBS Conference on*IEEE, 2013, p. 561-564.

Meigal AI, Rissanen S, Tarvainen M, Karjalainen P, Iudina-Vassel I, Airaksinen O, and Kankaanpää M. Novel parameters of surface EMG in patients with Parkinson's disease and healthy young and old controls. *Journal of Electromyography and Kinesiology* 19: e206-e213, 2009.

Mima T, and Hallett M. Corticomuscular coherence: a review. *Journal of Clinical Neurophysiology* 16: 501, 1999.

Nakagawa S, and Schielzeth H. A general and simple method for obtaining R2 from generalized linear mixed-effects models. *Methods in ecology and evolution* 4: 133-142, 2013.

Nawab SH, Chang S-S, and De Luca CJ. High-yield decomposition of surface EMG signals. *Clinical neurophysiology* 121: 1602-1615, 2010.

Negro F, and Farina D. Linear transmission of cortical oscillations to the neural drive to muscles is mediated by common projections to populations of motoneurons in humans. *The Journal of physiology* 589: 629-637, 2011.

Nordstrom MA, Fuglevand A, and Enoka R. Estimating the strength of common input to human motoneurons from the cross-correlogram. *The Journal of physiology* 453: 547-574, 1992.

Perez MA, Lundbye-Jensen J, and Nielsen JB. Changes in corticospinal drive to spinal motoneurones following visuo-motor skill learning in humans. *The Journal of physiology* 573: 843-855, 2006.

Perez MA, Soteropoulos DS, and Baker SN. Corticomuscular coherence during bilateral isometric arm voluntary activity in healthy humans. *Journal of neurophysiology* 107: 2154-2162, 2012.

Pierrot-Deseilligny E, and Burke D. *The circuitry of the human spinal cord: its role in motor control and movement disorders*. Cambridge University Press, 2005.

Pohja M, and Salenius S. Modulation of cortex-muscle oscillatory interaction by ischaemia-induced deafferentation. *Neuroreport* 14: 321-324, 2003.

Porter R, and Lemon R. *Corticospinal function and voluntary movement*. Oxford University Press, USA, 1993.

Powers RK, and Türker KS. Deciphering the contribution of intrinsic and synaptic currents to the effects of transient synaptic inputs on human motor unit discharge. *Clinical neurophysiology* 121: 1643-1654, 2010.

Richman JS, and Moorman JR. Physiological time-series analysis using approximate entropy and sample entropy. *American Journal of Physiology-Heart and Circulatory Physiology* 278: H2039-H2049, 2000.

Riddle CN, Edgley SA, and Baker SN. Direct and indirect connections with upper limb motoneurons from the primate reticulospinal tract. *Journal of neuroscience* 29: 4993-4999, 2009.

Ritter P, Moosmann M, and Villringer A. Rolandic alpha and beta EEG rhythms' strengths are inversely related to fMRI-BOLD signal in primary somatosensory and motor cortex. *Human brain mapping* 30: 1168-1187, 2009.

Schmied A, and Descarreaux M. Influence of contraction strength on single motor unit synchronous activity. *Clinical neurophysiology* 121: 1624-1632, 2010.
Schmied A, and Descarreaux M. Reliability of EMG determinism to detect changes in motor unit synchrony and coherence during submaximal contraction. *Journal of neuroscience methods* 196: 238-246, 2011.
Schmied A, Forget R, and Vedel J-P. Motor unit firing pattern, synchrony and coherence in a deafferented patient. *Frontiers in human neuroscience* 8: 2014.
Semmler JG, Kornatz KW, Dinenno DV, Zhou S, and Enoka RM. Motor unit synchronisation is enhanced during slow lengthening contractions of a hand muscle. *The Journal of physiology* 545: 681-695, 2002.
Semmler JG, Kornatz KW, and Enoka RM. Motor-unit coherence during isometric contractions is greater in a hand muscle of older adults. *Journal of neurophysiology* 90: 1346-1349, 2003.
Spinks RL, Kraskov A, Brochier T, Umilta MA, and Lemon RN. Selectivity for grasp in local field potential and single neuron activity recorded simultaneously from M1 and F5 in the awake macaque monkey. *Journal of neuroscience* 28: 10961-10971, 2008.
Taylor AM, and Enoka RM. Quantification of the factors that influence discharge correlation in model motor neurons. *Journal of neurophysiology* 91: 796-814, 2004.
Ushiyama J, Masakado Y, Fujiwara T, Tsuji T, Hase K, Kimura A, Liu M, and Ushiba J. Contraction level-related modulation of corticomuscular coherence differs between the tibialis anterior and soleus muscles in humans. *Journal of Applied Physiology* 112: 1258-1267, 2012.
Webber C, Schmidt M, and Walsh J. Influence of isometric loading on biceps EMG dynamics as assessed by linear and nonlinear tools. *Journal of Applied Physiology* 78: 814-822, 1995.
Williams ER, Soteropoulos DS, and Baker SN. Coherence between motor cortical activity and peripheral discontinuities during slow finger movements. *Journal of neurophysiology* 2009.
Witham CL, Riddle CN, Baker MR, and Baker SN. Contributions of descending and ascending pathways to corticomuscular coherence in humans. *The Journal of physiology* 589: 3789-3800, 2011.
Witham CL, Wang M, and Baker SN. Cells in somatosensory areas show synchrony with beta oscillations in monkey motor cortex. *European Journal of Neuroscience* 26: 2677-2686, 2007.
Witte M, Patino L, Andrykiewicz A, Hepp-Reymond MC, and Kristeva R. Modulation of human corticomuscular beta-range coherence with low-level static forces. *European Journal of Neuroscience* 26: 3564-3570, 2007.
Zoghi M, and Nordstrom MA. Progressive suppression of intracortical inhibition during graded isometric contraction of a hand muscle is not influenced by hand preference. *Experimental brain research* 177: 266-274, 2007.

Tables

Table 1. Mean (standard deviation) of detected and accepted motor units

	Constant Force				Increasing Force		Decreasing Force	
	10% MVC	20% MVC	30% MVC	40% MVC	10→ 20% MVC	20→ 30% MVC	20→ 10% MVC	30→ 20% MVC
Total MUs	27.3±7	26.2±6	26.6±7	28.9±6	28.5±8	31.3±8	26.2±7	25±6
Accepted MUs	20.9±5	20.6±5	20.9±5	22.0±5	17.0±5	18.3±4	16.0±4	15.9±4

Table 2. Mixed model ANOVA results for the constant force and two-force trials

(a)	Beta-band Motor Unit Coherence during Constant Force Trials				
Model Term	df1/2	F-Statistic	P-value		Semi-Partial R^2
Force	3/151	31.89	<0.001	***	0.22 [0.21, 0.23]
MFR	1/151	1.59	0.21		0.01 [0.00, 0.07]
MUnum	1/165	67.7	<0.001	***	0.28 [0.17, 0.38]
Marginal R^2	0.43	Conditional R^2	0.66		

(b)	Beta-band Motor Unit Coherence during Two-Force Trials				
Model Term	df1/2	F-Statistic	P-value		Semi-Partial R^2
Force	7/260	47.02	<0.001	***	0.31 [0.30, 0.32]
MFR	1/240	2.20	0.14		0.01 [0.00, 0.04]
MUnum	1/272	48.51	<0.001	***	0.13 [0.06, 0.20]
Marginal R^2	0.50	Conditional R^2	0.69		

Table 3. Repeated measures correlation results for the constant force and two-force trials

	Constant Force Trials				Two-Force Trials			
	SampEn		%DET		SampEn		%DET	
	r	p	r	p	r	p	r	p
Beta-band MU Coherence (15 – 35 Hz)	-0.29 [-0.43, -0.14]	<.001	0.32 [0.17, 0.46]	<.001	-0.53 [-0.61, -0.43]	<.001	0.48 [0.39, 0.57]	<.001
Alpha-band MU Coherence (8 – 12 Hz)	-0.35 [-0.49, -0.21]	<.001	0.44 [0.31, 0.56]	<.001	-0.53 [-0.61, -0.44]	<.001	0.56 [0.47, 0.63]	<.001

Legends to Figures and Tables

Table 1. Average number of motor unit detected during each trial, and the number of units used in further analysis, for the constant force and two-force trials.

Table 2. Mixed model ANOVA results (Type III) ANOVAs using the Kenward-Roger approximation for degrees of freedom investigating the effect of each fixed factor on the beta-band motor unit coherence. The degrees of freedom listed under df1/2 were rounded to the next integer. Values shown are for beta-band coherence during the (a) constant force trials and (b) two-force trials.

Table 3. The results of a repeated measures correlation between the nonlinear parameters (SampEn/%DET) and the motor unit coherence Bakdash and Marusich (2017). Correlations and confidence intervals were obtained for the beta-band (15-35 Hz) and alpha-band (8-12 Hz) motor unit coherence. Each p-value was corrected for multiple comparisons using the Benjamini-Hochberg procedure.

Figure 1. (a) Median and interquartile range of the fisher-transformed coherence values in the beta-band range across all subjects. Differences in MU coherence between force levels were tested with pairwise comparisons of least-square means using all trials (N = 171 trials, see Table 1 for average MU number per trial), while adjusting for the effect of MUnum and MFR. (b) Composite coherence spectrum across all subjects, averaged across all subjects and trials (in 2.5 Hz bins), *p < .05, **p < .01,***p < .001.

Figure 2. (a) The magnitude-squared coherence spectrum for a single subject, averaged across all trials (in 1 Hz bins) and (b) the motor unit mean firing rates as a function of the motor unit action potential size within a single representative trial at each force level (fit with a stretched exponential function).

Figure 3. (a) The power spectral density of two motor unit pulse trains for a representative 20%MVC trial, their respective firing rates (MU 1: interpulse interval (IPI) = 0.052 ± 0.013 s and MU 1: IPI = 0.085 ± 0.026 s), and the coherence estimate obtained for the motor unit pair. The power spectral density is presented for the summed motor unit pulse trains in the same trial in groups of (b) 6 MU, (c) and (d) 10 MUs, and (e) 20 MUs, alongside the composite motor unit coherence estimate for each group. In (e) the interpulse intervals of the raw pulse trains were shuffled to remove any correlation but maintain the same mean firing rates, and the coherence estimate was calculated on the reconstructed pulse trains with shuffled IPIs. (f) A schematic

1020 illustrating how a driving oscillation of a particular frequency could modulate motor unit
1021 activity, adapted from McAuley and Marsden (2000). A synchronous input can induce a motor
1022 unit to fire earlier than a similar unsynchronised input, so that the motor unit has a higher
1023 probability of firing with each 30 or 10 Hz input. An external periodic signal can thus modulate
1024 motor unit firing patterns to produce coherence peaks at frequencies distinct from the motor unit
1025 mean firing rates.

1026 Figure 4. Median and interquartile range of the fisher-transformed coherence values in the beta-
1027 band range during the first and second half of a trial with two contraction force levels. Both (a)
1028 increasing and (b) decreasing force trials are shown. (c) Changes in motor unit mean firing rates
1029 during the two force level trials. Differences in MU coherence and motor unit mean firing rate
1030 between force levels were tested with pairwise comparisons of least-square means using both
1031 the low and high force sections of all trials (N = 142 trials, see Table 1 for average MU number
1032 per trial), with differences in MU coherence adjusted for the effect of MUnum and MFR, *p <
1033 .05, **p < .01, ***p < .001.

1034 Figure 5. (a) The distribution of the fisher-transformed coherence values in the beta-band range
1035 for the 8 smallest MUs (low threshold) and the 8 largest MUs (high threshold) across all
1036 subjects at 40% MVC (data from each subject was normalised to minimise the contribution of
1037 inter-subject variance (Loftus and Masson 1994)) and (b) the distribution of the fisher-
1038 transformed coherence for a single trial in a representative subject at 20% MVC, with the
1039 coherence and MU mean firing rates calculated for three groups of 10 MUs arranged in order of
1040 size.

1041 Figure 6. (a) Median and interquartile range of the fisher-transformed coherence values in the
1042 beta-band range during the first and second half of the constant force contraction across all
1043 subjects, (b) median and standard deviation of the percentage determinism and the median
1044 frequency of the surface EMG signal, and (c) the surface EMG, motor unit mean firing rates and
1045 the wavelet coherence during a single force trial at 30% MVC in a representative subject. *p <
1046 .05, ***p < .001.

1047 Figure 7: (A) Sample cross-correlograms between pairs of motor unit pulse trains. Across all
1048 trials, approximately 58 ± 10% of MU pairs had a narrow or broad peak (of varying amplitude)
1049 centred at approximately zero lag in the cross-correlogram (green), 5 ± 4% had a dip or trough
1050 at zero lag (red) and 37 ± 10% showed no distinct peaks or troughs (blue). (B) The percentage
1051 of the motor unit pairs that exhibited a trough at zero lag in the cross-correlogram at each force
1052 level, for all subjects (median over all subjects shown in black). (C) Troughs could be
1053 artificially induced in the cross-correlogram for a motor unit pair by deleting co-incident firing

times in one motor unit (MU2) relative to the other reference unit (MU1). A broader, less-distinct peak in the correlogram was observed when firing times were shifted (by 3 ms or less) in MU2 relative to co-incident firings in MU1. (D) Changes in the coherence spectrum following the deletion of co-incident firings in selected motor units, for a trial in which no troughs were originally detected. Troughs were artificially induced in 1) 7.5% of all motor unit pairs (2/15 MUs indicated for removal) and 2) 10% of all motor unit pairs (3/15 MUs indicated for removal).

Figure 8. Median and interquartile range of the (a) sample entropy and (b) percentage determinism calculated from the surface EMG signal during the constant force trials at 10%, 20%, 30% and 40% MVC. Both (a) increasing and (b) decreasing force trials are shown. The sample entropy of the surface EMG signal was calculated for the first and second half of the trials with two contraction force levels, with both (c) increasing and (d) decreasing force trials shown. Differences in SampEn and %DET between force levels were tested with pairwise comparisons of least-square means using all constant force (N = 171 trials) and two-force trials (N = 142 trials, see Table 1 for average MU number per trial), *p < .05, **p < .01, ***p < .001.

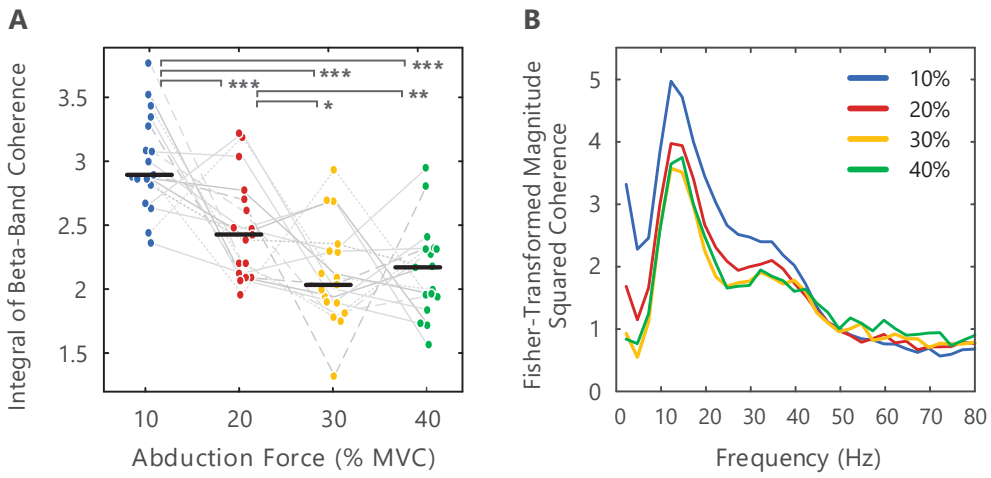
A
Integral of Beta-Band Coherence
3.5
3
2.5
2
1.5
***
***
***
*
**
10
20
30
40
Abduction Force (% MVC)
B
Fisher-Transformed Magnitude Squared Coherence
5
4
3
2
1
0
10%
20%
30%
40%
0
10
20
30
40
50
60
70
80
Frequency (Hz)

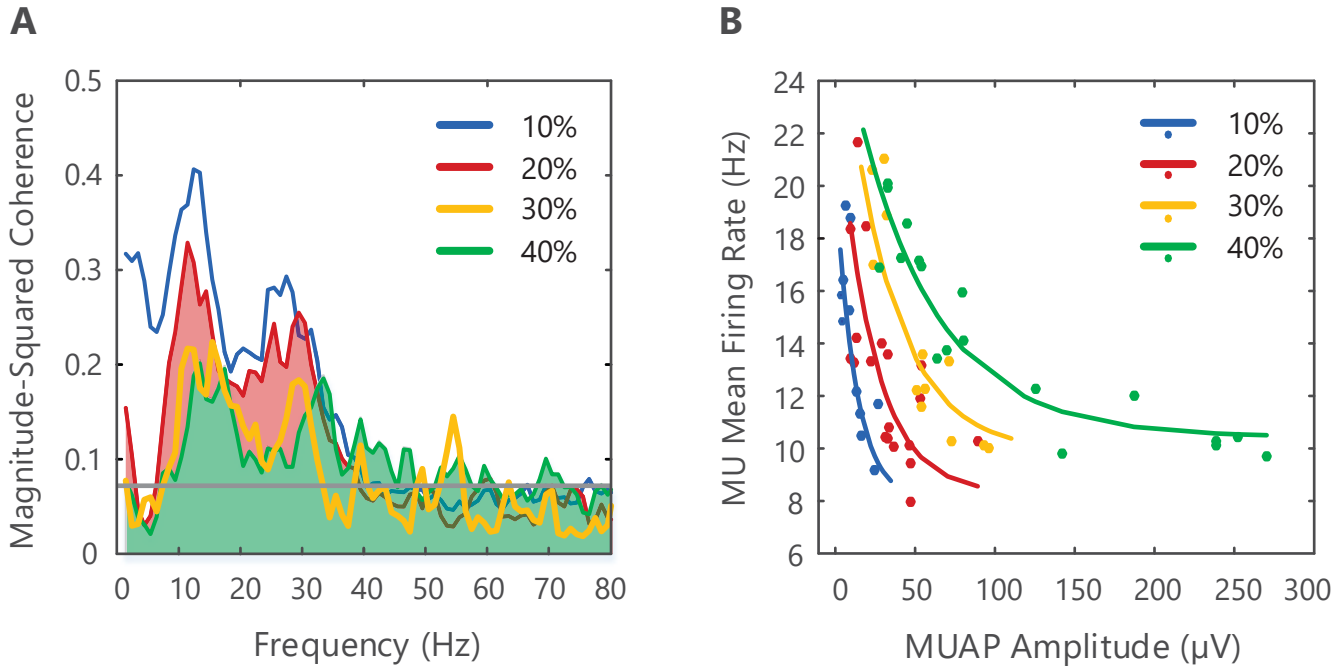
A
Magnitude-Squared Coherence
0.5
0.4
0.3
0.2
0.1
0
0
10
20
30
40
50
60
70
80
Frequency (Hz)
10%
20%
30%
40%
B
MU Mean Firing Rate (Hz)
24
22
20
18
16
14
12
10
8
6
0
50
100
150
200
250
300
MUAP Amplitude (μV)
10%
20%
30%
40%

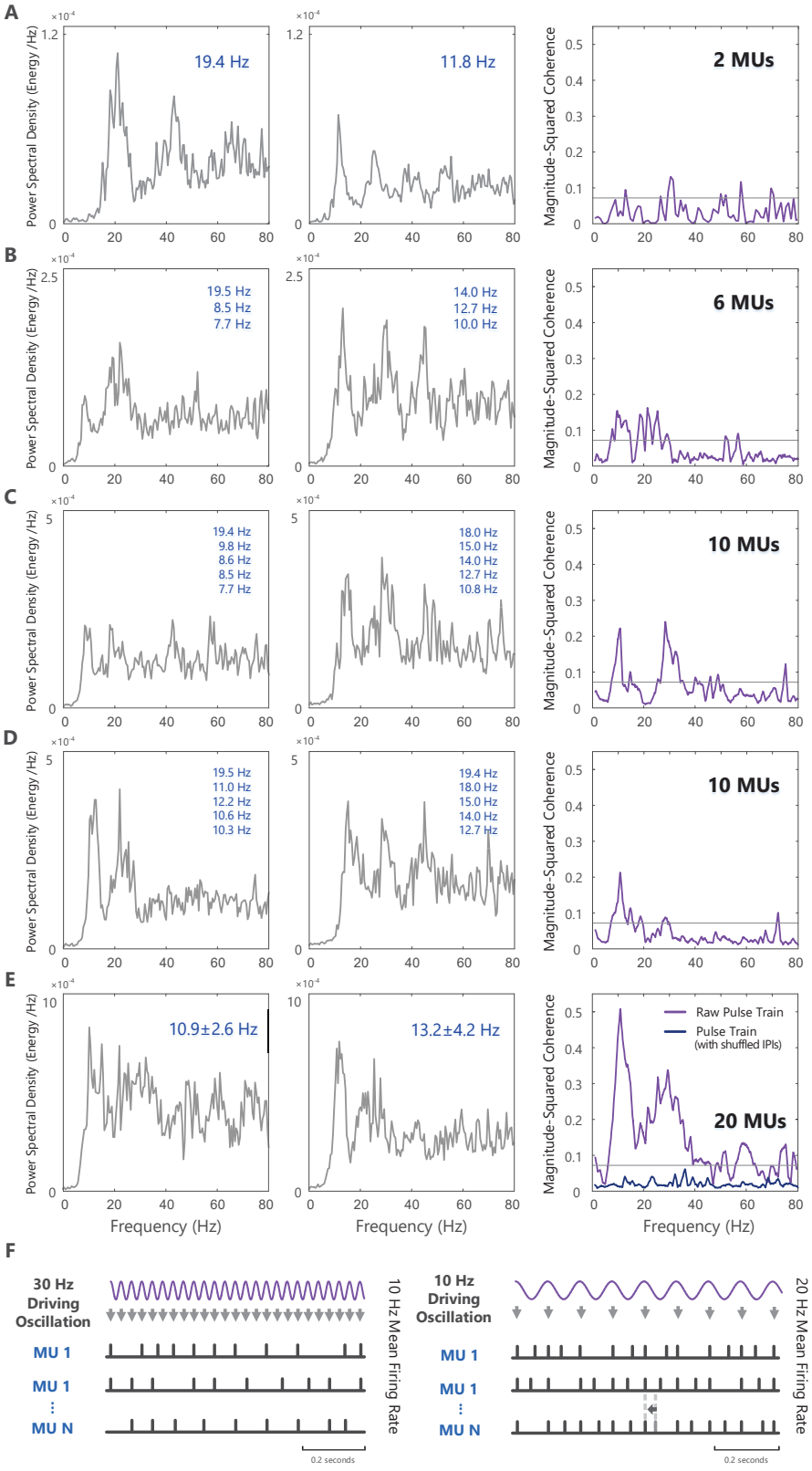
A
B
C
D
E
F
Power Spectral Density (Energy /Hz)
Magnitude-Squared Coherence
Frequency (Hz)
19.4 Hz
11.8 Hz
2 MUs
19.5 Hz
8.5 Hz
7.7 Hz
14.0 Hz
12.7 Hz
10.0 Hz
6 MUs
19.4 Hz
9.8 Hz
8.6 Hz
8.5 Hz
7.7 Hz
18.0 Hz
15.0 Hz
14.0 Hz
12.7 Hz
10.8 Hz
10 MUs
19.5 Hz
11.0 Hz
12.2 Hz
10.6 Hz
10.3 Hz
19.4 Hz
18.0 Hz
15.0 Hz
14.0 Hz
12.7 Hz
10 MUs
10.9±2.6 Hz
13.2±4.2 Hz
Raw Pulse Train
Pulse Train
(with shuffled IPIs)
20 MUs
30 Hz
Driving
Oscillation
MU 1
MU 1
MU N
10 Hz Mean Firing Rate
0.2 seconds
10 Hz
Driving
Oscillation
MU 1
MU 1
MU N
20 Hz Mean Firing Rate
0.2 seconds

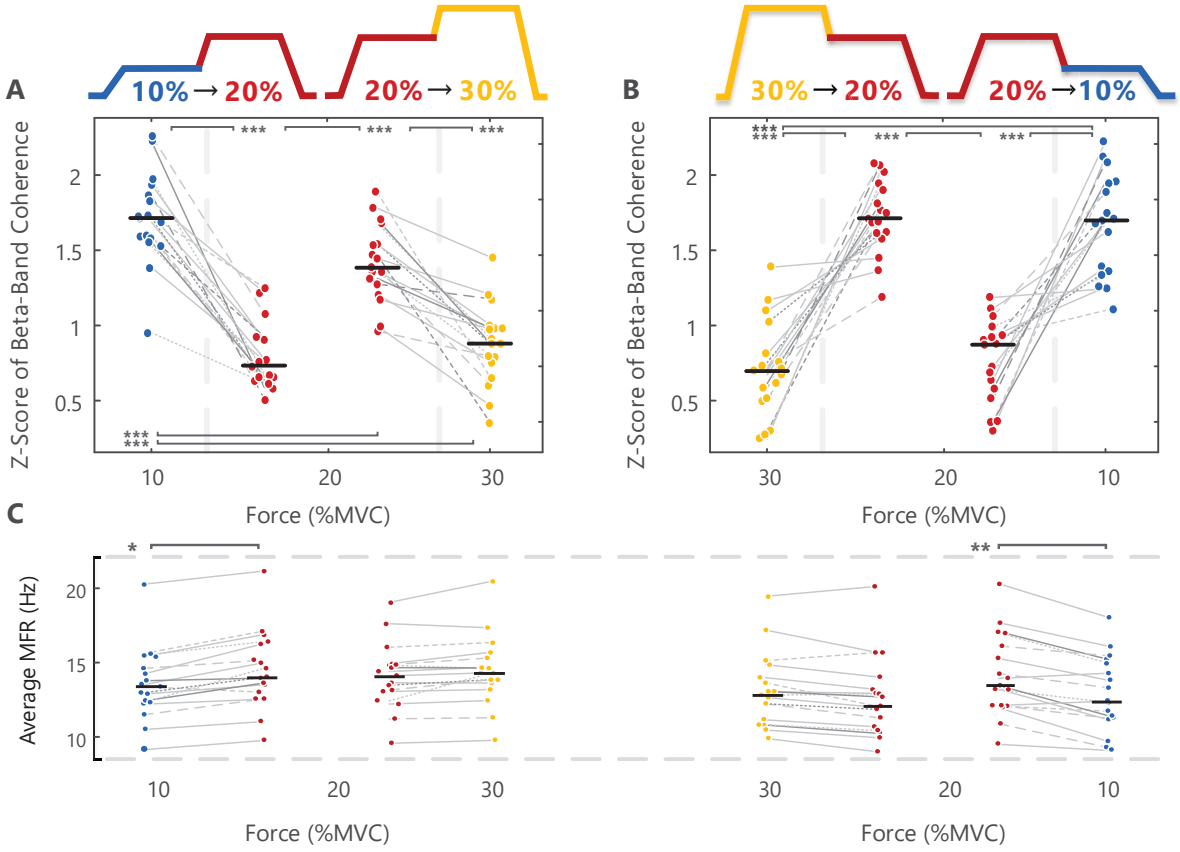
A
10% → 20%
20% → 30%
Z-Score of Beta-Band Coherence
Force (%MVC)
B
30% → 20%
20% → 10%
Z-Score of Beta-Band Coherence
Force (%MVC)
C
Average MFR (Hz)
Force (%MVC)
Force (%MVC)

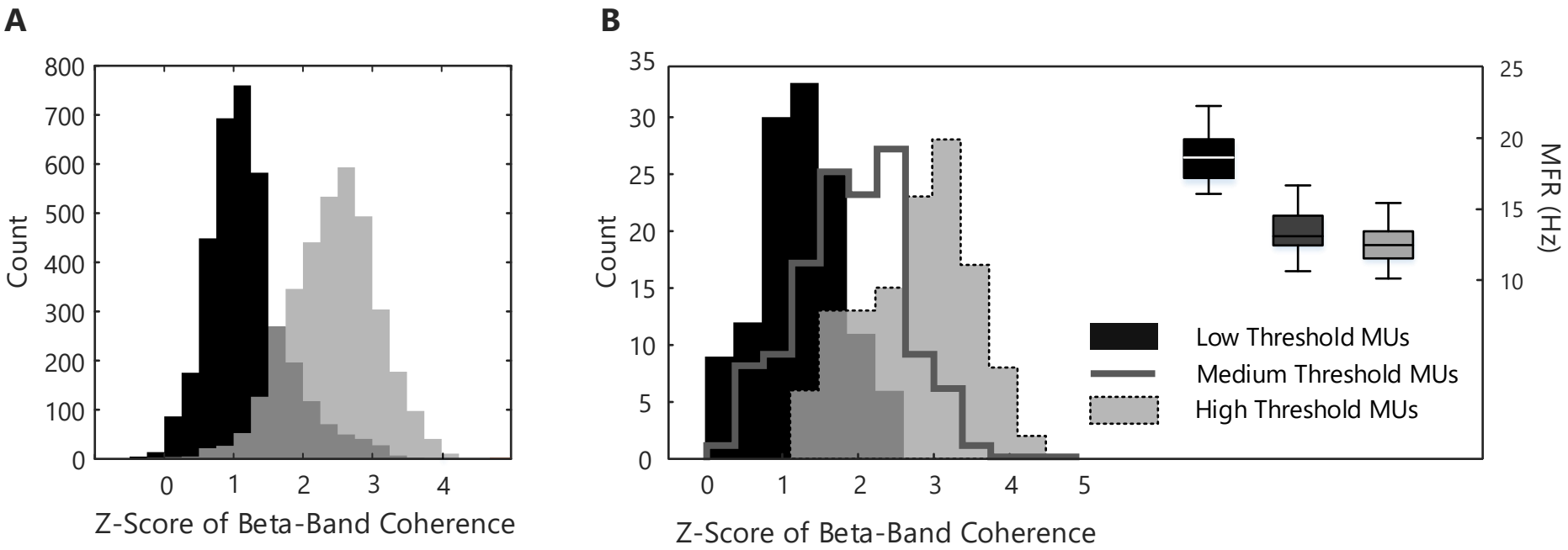
A
800
700
600
500
400
300
200
100
0
Count
0
1
2
3
4
Z-Score of Beta-Band Coherence
B
35
30
25
20
15
10
5
0
Count
0
1
2
3
4
5
Z-Score of Beta-Band Coherence
25
20
15
10
MFR (Hz)
Low Threshold MUs
Medium Threshold MUs
High Threshold MUs

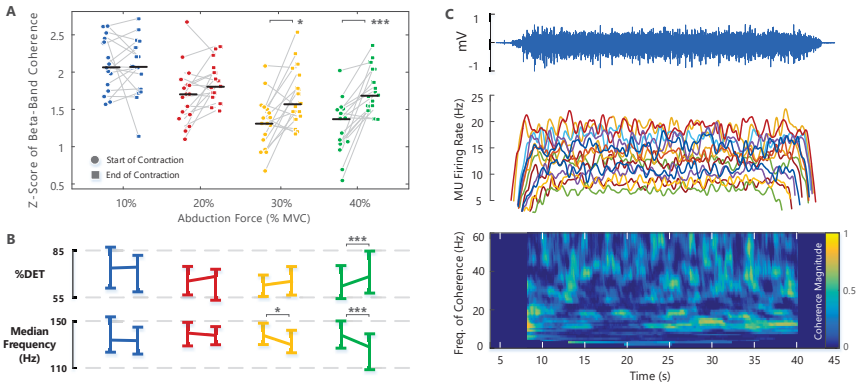
A
Z-Score of Beta-Band Coherence
2.5
2
1.5
1
0.5
*
***
Start of Contraction
End of Contraction
10%
20%
30%
40%
Abduction Force (% MVC)
B
%DET
85
55
***
Median Frequency (Hz)
150
110
*
***
C
mV
1
-1
MU Firing Rate (Hz)
25
20
15
10
5
Freq. of Coherence (Hz)
60
40
20
0
Coherence Magnitude
1
0.5
0
5
10
15
20
25
30
35
40
45
Time (s)

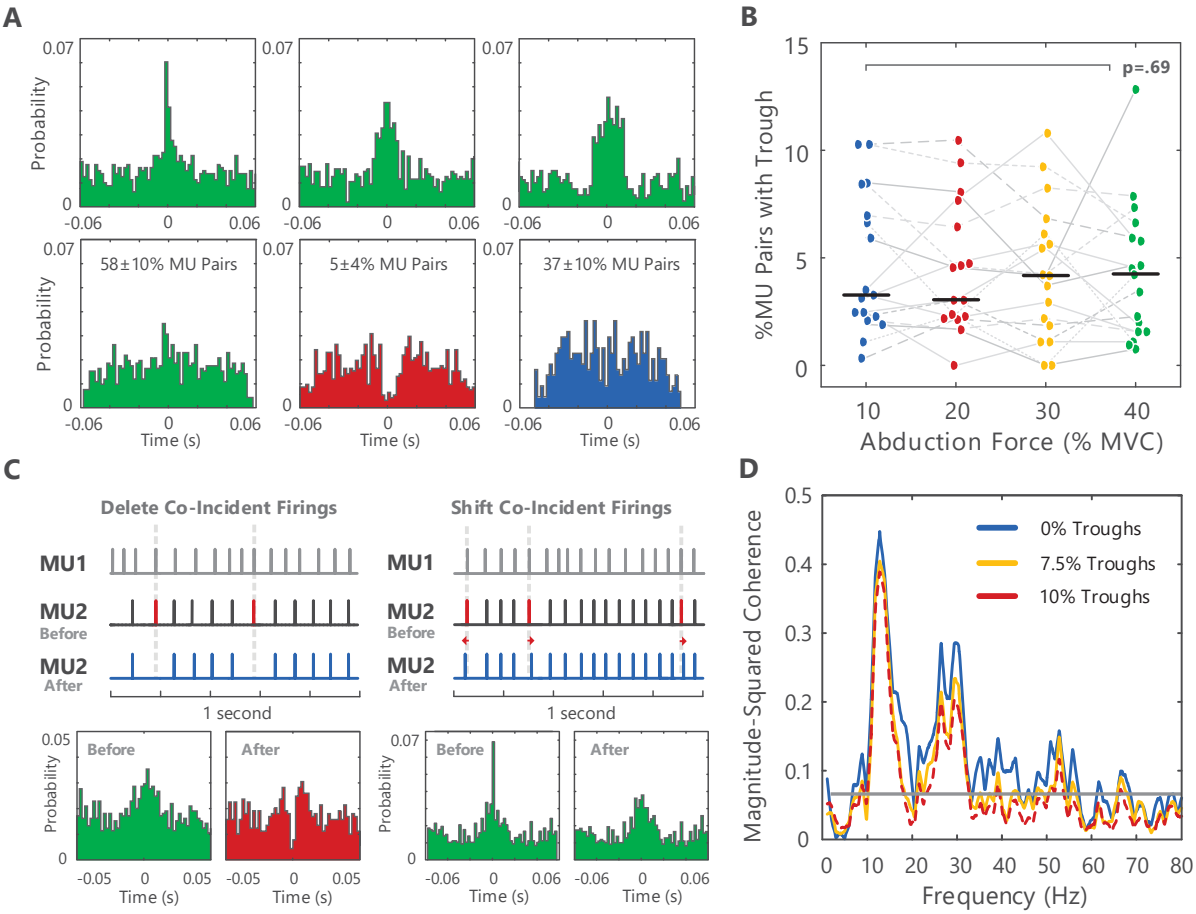
A
Probability
0.07
0
-0.06
0
0.06
58±10% MU Pairs
5±4% MU Pairs
37±10% MU Pairs
Time (s)
B
%MU Pairs with Trough
p=.69
Abduction Force (% MVC)
C
Delete Co-Incident Firings
Shift Co-Incident Firings
MU1
MU2
Before
After
1 second
Probability
Time (s)
D
Magnitude-Squared Coherence
0% Troughs
7.5% Troughs
10% Troughs
Frequency (Hz)

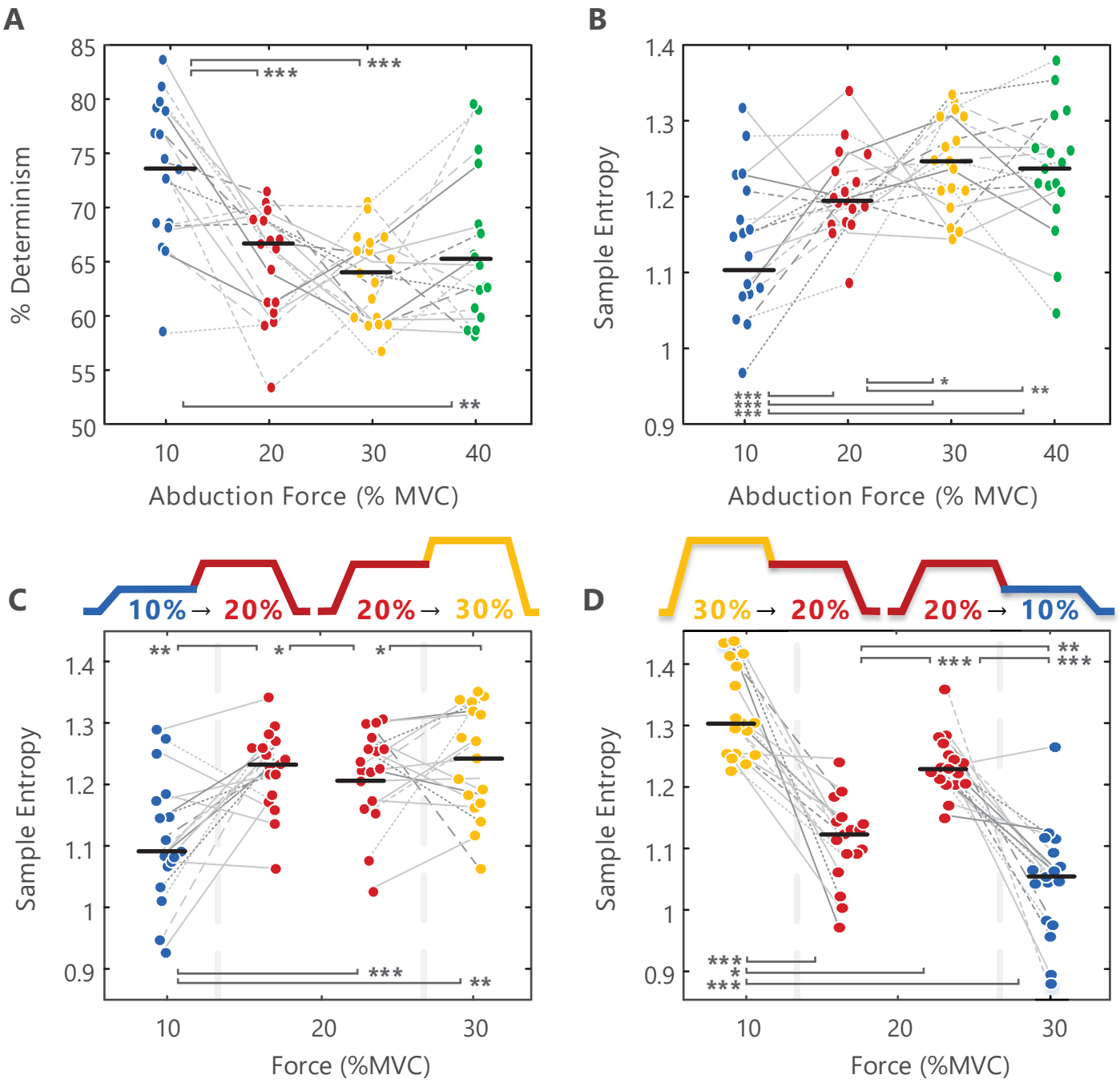
A
% Determinism
Abduction Force (% MVC)
B
Sample Entropy
Abduction Force (% MVC)
C
10% → 20%
20% → 30%
Sample Entropy
Force (%MVC)
D
30% → 20%
20% → 10%
Sample Entropy
Force (%MVC)